ARMY RESEARCH LABORATORY

A Finite Point Process Approach to Multi-Target Localization

by Jemin George and Lance M. Kaplan

ARL-TR-6659 September 2013

NOTICES

Disclaimers

The findings in this report are not to be construed as an official Department of the Army position unless so designated by other authorized documents.

Citation of manufacturer’s or trade names does not constitute an official endorsement or approval of the use thereof.

Destroy this report when it is no longer needed. Do not return it to the originator.

Army Research Laboratory

Adelphi, MD 20783-1197

ARL-TR-6659 **September 2013**

A Finite Point Process Approach to Multi-Target Localization

Jemin George and Lance M. Kaplan

Sensors and Electron Devices Directorate, ARL

REPORT DOCUMENTATION PAGE

Form Approved
OMB No. 0704-0188

1. REPORT DATE *(DD-MM-YYYY)*	2. REPORT TYPE	3. DATES COVERED (From - To)
September 2013	Final	October 2012-September 2013

4. TITLE AND SUBTITLE
A Finite Point Process Approach to Multi-Target Localization

5a. CONTRACT NUMBER

5b. GRANT NUMBER

5c. PROGRAM ELEMENT NUMBER

6. AUTHOR(S)
Jemin George and Lance M. Kaplan

5d. PROJECT NUMBER

5e. TASK NUMBER

5f. WORK UNIT NUMBER

7. PERFORMING ORGANIZATION NAME(S) AND ADDRESS(ES)
U.S. Army Research Laboratory
ATTN: RDRL-SES-A
2800 Powder Mill Road, Adelphi MD 20783

8. PERFORMING ORGANIZATION REPORT NUMBER
ARL-TR-6659

9. SPONSORING/MONITORING AGENCY NAME(S) AND ADDRESS(ES)

10. SPONSOR/MONITOR'S ACRONYM(S)

11. SPONSOR/MONITOR'S REPORT NUMBER(S)

12. DISTRIBUTION/AVAILABILITY STATEMENT
Approved for public release; distribution is unlimited.

13. SUPPLEMENTARY NOTES
Author email: <jemin.george.civ@mail.mil>

14. ABSTRACT
A finite point process approach to multi-target localization from a transient signal is presented. After modeling the measurements as a Poisson point process, we propose a twofold scheme that includes an expectation maximization algorithm to estimate the target locations for a given number of targets and an information theoretic algorithm to select the target model, i.e., number of targets. Similar to the finite point process solution for the multi-target tracking, i.e., the probability hypothesis density filter, the proposed localization scheme does not require solving the data association problem and can account for clutter noise as well as missed detection. The optimal subpattern assignment metric is used to assess the performance and accuracy of the proposed localization algorithm. Implementation of the proposed algorithm on synthetic data yields desirable results. The proposed algorithm is then applied to multi-shooter localization problem using acoustic gunfire detection systems.

15. SUBJECT TERMS Poisson point process, finite point process, multi-target localization, expectation maximization algorithm, information theoretic algorithm, acoustic gunfire detection systems

16. SECURITY CLASSIFICATION OF:			17. LIMITATION OF ABSTRACT	18. NUMBER OF PAGES	19a. NAME OF RESPONSIBLE PERSON
a. REPORT	b. ABSTRACT	c. THIS PAGE			Jemin George
Unclassified	Unclassified	Unclassified	UU	52	19b. TELEPHONE NUMBER (*Include area code*) 301-394-3977

Standard Form 298 (Rev. 8/98)
Prescribed by ANSI Std. Z39.18

Contents

List of Figures

List of Tables

1. Introduction

This report considers the problem of multi-target localization using transient signals from a single-sensor as well as multi-sensor point of view. Here it is assumed that target identification is not possible, and therefore, no association between measurements and targets are available. Furthermore, the number of targets in the surveillance region is unknown. Additionally, due to the limited range of the sensors, missed detections can occur and the presence of clutter can induce false alarms. An example of such a scenario is shooter localization using a network of acoustic gunfire detection systems (GDSs) (*1*). The individual GDSs composed of a passive array of microphones are able to localize a gunfire event by measuring the direction of arrival for both the acoustic wave generated by the muzzle blast and the shockwave generated by the supersonic bullet (*2–5*). Due to echo, reverberation, and the dissipative nature of the acoustic signal, missed detections and false alarms are prevalent in acoustic source localization. Furthermore, due to the transient nature of the event, continuous observations are not available and recursive Bayesian tracking schemes cannot be employed.

Conventional multi-target tracking (MTT) approaches like Multiple Hypothesis Tracking (MHT) (*6, 7*) or the Joint Probability Data Association (JPDA) filter (*8, 9*), which address the data-association problem, either are too computationally demanding or cannot be applied to the transient event localization problem since these approaches require persistent measurement signals and a fixed number of targets. In MHT, all possible combinations of tracks and data associations are exhaustively evaluated; therefore, it is an impractical scheme since the number of mappings between data and targets will grow exponentially with the number of targets (*10, 11*). Though more efficient than MHT, JPDA methods are not optimal since the detection is performed separately from tracking and cannot initiate tracks at low signal-to-clutter ratios (*12*). A multi-target extension of the simultaneous localization and mapping (SLAM) problem for streaming data is presented by Garcia-Fernandez et al. (*13*). The multi-target simultaneous localization and mapping (MSLAM) scheme is based on the parallel partition particle filter and it outperforms the well-known FastSLAM (*14*) when there are multiple targets in the surveillance area. Jensfelt and Kristensen (*15*) discuss an extension of the MHT, known as the multi-hypothesis localization (MHL), for mobile robot localization. The MHL uses a multi-hypothesis Kalman filter along with a probabilistic formulation of hypothesis correctness to generate and track Gaussian hypotheses. However, almost all of the MTT techniques are recursive algorithms that require persistent observations and are futile in dealing with transient

signals.

A finite point process approach known as the probability hypothesis density (PHD) filter, introduced by Mahler (*16*), allows a more tractable implementation of multi-target tracking approaches since it only propagates the first-order moment of the multi-target density. Moreover, the PHD filter is able to handle a time-varying number of targets, missed detections, and false alarms. Though the track labeling problem is not considered in the PHD filter, a track labeling method combined with the PHD approach, is proposed by Lin et al. (*17*) for multi-target tracking. Since the implementation of an exact PHD filter is intractable, a sequential Monte Carlo (SMC) or particle filtering approach (*18*) and the Gaussian sum filtering scheme (*19*) have been devised to approximate the PHD filter. Convergence properties for the particle PHD filter and Gaussian mixture PHD filter are presented in references (*20*) and (*21*), respectively. An SMC implementation of a finite set statistical filter for the localization of an unknown number of speakers in a multipath environment using time difference of arrival (TDOA) measurements has also been proposed (*18, 22–24*). Similar to traditional MTT algorithms, the PHD filter is a recursive Bayesian approach, which also requires persistent observations for track update. A finite point process approach to maximum likelihood based multi-target localization of an unknown number of targets from transient signals has not been considered yet.

Traditionally, multi-target localization involves the maximum likelihood based approach, where the selected model yields the maximum likelihood of observing the given data across a possible number of targets and all possible target-data associations. As the number of sensors increases, the possible combination of target-data associations dramatically increases, and the problem often becomes intractable. Development of a multi-target detection and localization scheme based on a probabilistic framework known as modeling field theory (MFT) is presented by Deming and Perlovsky (*25*). Though the computational complexity of a MFT-based approach scales linearly with the size of the problem, it involves an iterative scheme similar to the expectation maximization (EM) and an ad-hoc likelihood ratio test is needed to prune the number of targets. An iterative maximum likelihood optimization technique based on a modified deterministic annealing EM (MDAEM) algorithm for multi-target localization and velocity estimation using TDOAs is given by Carevic (*26*). Since the MDAEM algorithm is executed for an assumed number of targets, Carevic (*27*) provides a systematic approach for determining which of the target models estimated by the MDAEM algorithm are related to the true targets. Both the MFT-based approach and the MDAEM algorithm require that the assumed number of targets is greater than or equal to the true number of targets. Also, the measurements are only assumed to contain clutter/false alarms and the problem of missed detection is not considered.

For the multi-target localization problem considered here, we use the frequentist counterpart to the Bayesian filtering approach, i.e., the maximum likelihood algorithm. The localization problem is formulated in two dimensions and the measurements considered here are the range and the bearing to the targets. Each sensor acquires several range and bearing measurement pairs and the proposed algorithm estimates the number of targets and their corresponding locations based on the erroneous measurements. The number of targets is certainly different from the number of measurements due to clutter and missed detection. The proposed approach is a twofold scheme that includes an EM algorithm to estimate the target locations for a given number of targets and an information theoretic algorithm to select the target model, i.e., number of targets and their locations. The main advantage of the proposed scheme is that it scales linearly with the size of the problem and avoids the curse of dimensionality associated with the traditional MHT-based multi-target localization scheme. For example, if there are N targets, S sensors, and m measurements per sensor, the computational complexity for the proposed scheme is in the order of $O\left(NSm\right)$ while the computational complexity for the traditional scheme is in the order of $O\left(N^{Sm}\right)$. Unlike the methods used by Deming and Perlovsky (*25*) and Carevic (*26*), the proposed approach accounts for probability of detection and missed detection along with clutter and false alarms.

The structure of this report is as follows: formulation of multi-target localization problem and the corresponding solution for the single-sensor scenario are presented in sections 2, and 3, respectively. A numerical example demonstrating the single-sensor algorithm is presented in section 4. Formulation of multi-target localization problem and the corresponding solution for the multi-sensor scenario is presented in sections 5, and 6, respectively. Numerical simulation demonstrating the multi-sensor algorithm are presented in section 7. Section 8 presents the results obtained from implementing the proposed algorithm on experimental data. Finally, Section 9 concludes the report and discusses the current research challenges.

2. Problem Formulation

Consider a two-dimensional (2-D) scenario where there are N targets located in $\mathbb{R}^2$. The target locations are denoted as

$$\left(\mathrm{T}_1,\, \mathrm{T}_2,\, \ldots,\, \mathrm{T}_N\right) = \left(\begin{bmatrix} T_{x_1} \\ T_{y_1} \end{bmatrix},\, \begin{bmatrix} T_{x_2} \\ T_{y_2} \end{bmatrix},\, \ldots,\, \begin{bmatrix} T_{x_N} \\ T_{y_N} \end{bmatrix} \right). \tag{1}$$

Due to clutter and miss detection, the number of targets and the target location set that may

induce a measurement are jointly modeled as a finite point process known as the Poisson Point Process (PPP) (*28*). A realization of this PPP, $\boldsymbol{\Xi}$, is denotes as

$$\boldsymbol{\xi} = \left(m, \left\{ \begin{bmatrix} t_{x_1} \\ t_{y_1} \end{bmatrix}, \begin{bmatrix} t_{x_2} \\ t_{y_2} \end{bmatrix}, \ldots, \begin{bmatrix} t_{x_m} \\ t_{y_m} \end{bmatrix} \right\} \right) = (m, \{\mathbf{t}_1, \mathbf{t}_2, \ldots, \mathbf{t}_m\}) . \tag{2}$$

The points in the PPP, i.e., $\mathbf{t}$, occur in a state space $\mathcal{S} = \mathbb{R}^2$ and the realizations of the PPP is defined in a bounded subset $\mathcal{R} \subset \mathcal{S}$. It is assumed that $\mathbf{T} = (\mathrm{T}_1, \mathrm{T}_2, \ldots, \mathrm{T}_N) \in \mathcal{R}$. In a PPP, the points $\mathbf{t}_i$ are not necessarily distinct and their order is irrelevant. The PPP is fully parameterized by the intensity function:

$$\lambda(\mathbf{t}) = \sum_{i=1}^{N} p^D(\mathbf{t})\, \delta(\mathbf{t} - \mathrm{T}_i), \tag{3}$$

where $\delta(\cdot)$ is the Dirac delta function, and $p^D(\cdot)$ represents the probability of detection. The number of points in the PPP, $\boldsymbol{\Xi}$, is determined by sampling the discrete Poisson random variable M with probability mass function (pmf):

$$p_M(m) = \frac{\left(\int_{\mathcal{R}} \lambda(\mathbf{t}) d\mathbf{t}\right)^m}{m!} \exp\left\{ - \int_{\mathcal{R}} \lambda(\mathbf{t}) d\mathbf{t} \right\}. \tag{4}$$

The m points, $\mathbf{t}_j \in \mathcal{R},\ j = 1, \ldots, m$, are defined as i.i.d. samples of a random variable $\mathbf{T}$ on $\mathcal{R}$ with probability density function (pdf):

$$p_{\mathbf{T}}(\mathbf{t}) = \frac{\lambda(\mathbf{t})}{\int_{\mathcal{R}} \lambda(\mathbf{t}) d\mathbf{t}}. \tag{5}$$

The number of targets and their locations are unknown, but a sensor located at $\begin{bmatrix} S_x & S_y \end{bmatrix}^T$ is able to observe the range and bearing to the targets. The measurement equation is, $\forall j = 1, \ldots, m$,

$$\mathbf{z}_j = \mathbf{h}(t_{x_j}, t_{y_j}) + \mathbf{w}_j, \Rightarrow \begin{bmatrix} r_j \\ \phi_j \end{bmatrix} = \begin{bmatrix} \sqrt{(t_{x_j} - S_x)^2 + (t_{y_j} - S_y)^2} \\ \arctan((t_{y_j} - S_y)/(t_{x_j} - S_x)) \end{bmatrix} + \begin{bmatrix} w_{r_j} \\ w_{\phi_j} \end{bmatrix}. \tag{6}$$

The noise $\mathbf{w}_j$ is assumed to be i.i.d. samples of Gaussian, zero mean process with variance $\Sigma_{\mathbf{w}} = \begin{bmatrix} \sigma_r^2 & 0 \\ 0 & \sigma_\theta^2 \end{bmatrix}$. Thus, the likelihood can be written as

$$l(\mathbf{z}|\mathbf{t}) = \mathcal{N}\left(\mathbf{z} \,|\, \mathbf{h}(\mathbf{t}), \Sigma_{\mathbf{w}} \right). \tag{7}$$

Let's assume that the each point $\mathbf{t}_j$ in the PPP realization $\boldsymbol{\xi}$ is observed by the sensor and subsequently, the sensor generates a measurement $\mathbf{z}_j \in \mathcal{T} \subset \mathbb{R}^2$. Let $\boldsymbol{\psi} = (m, \{\mathbf{z}_1, \ldots, \mathbf{z}_m\})$, then $\boldsymbol{\psi}$ is a realization of a PPP, $\boldsymbol{\Psi}$,defined on the space $\mathcal{T}$, with intensity

$$\nu(\mathbf{z}) = \int_{\mathcal{R}} l(\mathbf{z}|\mathbf{t})\lambda(\mathbf{t})d\mathbf{t} = \sum_{i=1}^{N} p^D(\mathrm{T}_i)\,\mathcal{N}\,(\,\mathbf{z}\,|\,\mathbf{h}(\mathrm{T}_i), \Sigma_{\mathbf{w}}) + \nu_{cl}(\mathbf{z}), \tag{8}$$

where $\nu_{cl}(\mathbf{z})$ is the clutter intensity. Thus the measured points are modeled as either samples from one of the N Gaussian densities or from the clutter intensity. Now the localization problem can be formally defined as follows:
Given $\boldsymbol{\psi} = (m, \{\mathbf{z}_1, \ldots, \mathbf{z}_m\})$, a realization of the PPP, $\boldsymbol{\Psi}$, and the clutter intensity $\nu_{cl}(\mathbf{z})$, find an estimate of the number of targets, N, target locations, $\mathrm{T}_1, \mathrm{T}_2, \ldots, \mathrm{T}_N$, and the corresponding probability of detection, $p^D(\mathrm{T}_i)$.

---

3. Proposed Single-Sensor Solution

The proposed twofold solution to the problem defined in the previous section consist of an EM algorithm to estimate the target locations for a given model for the intensity and a penalized log likelihood based information criteria to select the appropriate model. Here, the only difference in the intensity model is the number of Gaussian components in each model and their corresponding locations. Details of the twofold solution is given next.

3.1 EM Method

Assume the model is known, i.e., the number of targets is given. Given the number of targets, N, the intensity $\nu(\mathbf{z}\,|\,\mathbf{T})$ is the superposition of N weighted Gaussian components along with the clutter intensity:

$$\nu(\mathbf{z}\,|\,\mathbf{T}) = \sum_{i=1}^{N} p^D(\mathrm{T}_i)\,\mathcal{N}\,(\,\mathbf{z}\,|\,\mathbf{h}(\mathrm{T}_i),\,\Sigma_{\mathbf{w}}\,) + \nu_{cl}(\mathbf{z}\,|\,\mathbf{T}), \tag{9}$$

where the parameter vector of the i-th component is T_i and $\mathbf{T} = (\mathrm{T}_1, \mathrm{T}_2, \ldots, \mathrm{T}_N)$.

3.1.1 E - Step

The natural choice of the "missing data" are the conditionally independent random indices k_j, $k_j \in \{\emptyset, 1, 2, \ldots, N\}$, that identify which of the Gaussian components generated the

measurement $\mathbf{z}_j$. Here $k_j = \emptyset$ indicates that the measurement is generated by clutter. Let

$$\mathbf{z}_c = \{m, (\mathbf{z}_1, k_1), \ldots, (\mathbf{z}_m, k_m)\} \tag{10}$$

denote the complete data. For $i \in \{\emptyset, 1, 2, \ldots, N\}$, let

$$\mathbf{z}_c(i) = \{(\mathbf{z}_j, k_j) \,:\, k_j = i\}. \tag{11}$$

Let $n_c(i) \geq 0$ denote the number of indices j such that $k_j = i$, and let

$$\psi_c(i) = \{\, n_c(i),\, \mathbf{z}_c(i) \,\}\,. \tag{12}$$

It follows from the definition of k_j that $\psi_c(i)$ is a realization of the PPP whose intensity is

$$\psi_c(i) \sim \begin{cases} p^D(\mathrm{T}_i)\, \mathcal{N}\,(\,\mathbf{z} \,|\, \mathbf{h}(\mathrm{T}_i),\, \Sigma_{\mathbf{w}}\,)\,, & \text{if } i \in \{1, 2, \ldots, N\}; \\ \nu_{cl}(\mathbf{z} \,|\, \mathbf{T}), & \text{if } i = \emptyset. \end{cases} \tag{13}$$

Now only considering the first scenario, $i \in \{1, 2, \ldots, N\}$, the pdf of $\psi_c(i)$ can be written as

$$p\,(\psi_c(i) \,|\, \mathbf{T}) = \exp\left(- \int_{\mathcal{T}} p^D(\mathrm{T}_i)\, \mathcal{N}\,(\,\mathbf{z} \,|\, \mathbf{h}(\mathrm{T}_i),\, \Sigma_{\mathbf{w}}\,)\, d\mathbf{z} \right) \prod_{j:k_j=i} p^D(\mathrm{T}_i)\, \mathcal{N}\,(\,\mathbf{z}_j \,|\, \mathbf{h}(\mathrm{T}_i),\, \Sigma_{\mathbf{w}}\,) \tag{14}$$

and

$$p\,(\psi_c(\emptyset) \,|\, \mathbf{T}) = \exp\left(- \int_{\mathcal{T}} \nu_{cl}(\mathbf{z} \,|\, \mathbf{T}) d\mathbf{z} \right) \prod_{j:k_j=\emptyset} \nu_{cl}(\mathbf{z}_j \,|\, \mathbf{T}) \tag{15}$$

Since the superposed components are independent, we have

$$\begin{aligned} p\,(\mathbf{z}_c \,|\, \mathbf{T}) &= p\,(\psi_c(\emptyset) \,|\, \mathbf{T})\, p\,(\psi_c(1) \,|\, \mathbf{T})\, p\,(\psi_c(2) \,|\, \mathbf{T}) \ldots p\,(\psi_c(N) \,|\, \mathbf{T}) \\ &= \exp\left(- \int_{\mathcal{T}} \nu(\mathbf{z} \,|\, \mathbf{T})\, d\mathbf{z} \right) \prod_{j:k_j \neq \emptyset} p^D(\mathrm{T}_{k_j})\, \mathcal{N}\left(\,\mathbf{z}_j \,|\, \mathbf{h}(\mathrm{T}_{k_j}),\, \Sigma_{\mathbf{w}}\,\right) \prod_{j:k_j=\emptyset} \nu_{cl}(\mathbf{z}_j \,|\, \mathbf{T}) \end{aligned}$$

The log likelihood function of $\mathbf{T}$ given $\mathbf{z}_c$ is

$$\begin{aligned} \mathfrak{L}\,(\mathbf{T} \,|\, \mathbf{z}_c) = - \int_{\mathcal{T}} \nu(\mathbf{z} \,|\, \mathbf{T})\, d\mathbf{z} + \sum_{j:k_j \neq \emptyset} \log\, p^D(\mathrm{T}_{k_j}) + \sum_{j:k_j \neq \emptyset} \log\, \mathcal{N}\left(\,\mathbf{z}_j \,|\, \mathbf{h}(\mathrm{T}_{k_j}),\, \Sigma_{\mathbf{w}}\,\right) \\ + \sum_{j:k_j=\emptyset} \log\, \nu_{cl}(\mathbf{z}_j \,|\, \mathbf{T}) \end{aligned} \tag{16}$$

Note that the conditional pdf of the missing data, $(k_1, \ldots, k_m)$, given $\mathbf{T}$ and $\mathbf{z}$ can be written as

$$\begin{aligned} p\left(k_1, \ldots, k_m \,|\, \mathbf{z}, \mathbf{T}\right) &= \frac{p\left(\mathbf{z}_c \,|\, \mathbf{T}\right)}{p\left(\mathbf{z} \,|\, \mathbf{T}\right)} \\ &= \prod_{j:k_j \neq \emptyset} \frac{p^D(\mathrm{T}_{k_j})\, \mathcal{N}\left(\mathbf{z}_j \,|\, \mathbf{h}(\mathrm{T}_{k_j}),\, \Sigma_{\mathbf{w}}\right)}{\nu(\mathbf{z}_j \,|\, \mathbf{T})} \prod_{j:k_j = \emptyset} \frac{\nu_{cl}(\mathbf{z}_j \,|\, \mathbf{T})}{\nu(\mathbf{z}_j \,|\, \mathbf{T})} \end{aligned}$$

Invoking the Poisson Gambit, $p\left(k_1, \ldots, k_m \,|\, \mathbf{z}, \mathbf{T}\right)$ can be written as

$$p\left(k_1, \ldots, k_m \,|\, \mathbf{z}, \mathbf{T}\right) = p\left(k_1 \,|\, \mathbf{z}, \mathbf{T}\right) p\left(k_2 \,|\, \mathbf{z}, \mathbf{T}\right) \ldots p\left(k_m \,|\, \mathbf{z}, \mathbf{T}\right) \tag{17}$$

where the individual pdfs can be written as

$$p\left(k_j \,|\, \mathbf{z}, \mathbf{T}\right) = \begin{cases} \frac{p^D(\mathrm{T}_{k_j})\, \mathcal{N}\left(\mathbf{z}_j \,|\, \mathbf{h}(\mathrm{T}_{k_j}),\, \Sigma_{\mathbf{w}}\right)}{\nu(\mathbf{z}_j \,|\, \mathbf{T})}, & \text{if } k_j \neq \emptyset; \\ \frac{\nu_{cl}(\mathbf{z}_j \,|\, \mathbf{T})}{\nu(\mathbf{z}_j \,|\, \mathbf{T})}, & \text{else.} \end{cases} \tag{18}$$

Let $n = 0, 1, \ldots$ denote the EM iteration index, and let the current feasible value of $\mathbf{T}$ be $\mathbf{T}^{(n)} = \left(\mathrm{T}_1^{(n)}, \ldots, \mathrm{T}_N^{(n)}\right)$. Now the EM auxiliary function is the conditional expectation

$$\begin{aligned} Q\left(\mathbf{T} \,\middle|\, \mathbf{T}^{(n)}\right) &= E_{k_1,\ldots,k_m, \,\middle|\, \mathbf{z}, \mathrm{T}^{(n)}} \left[\mathfrak{L}\left(\mathbf{T} \,|\, \mathbf{z}_c\right) \,\middle|\, \mathbf{z}, \mathbf{T}^{(n)}\right] \\ &= \sum_{k_1=\emptyset}^{N} \cdots \sum_{k_m=\emptyset}^{N} \mathfrak{L}\left(\mathbf{T} \,|\, \mathbf{z}_c\right) \prod_{j:k_j \neq \emptyset} \frac{p^D(\mathrm{T}_{k_j})\, \mathcal{N}\left(\mathbf{z}_j \,|\, \mathbf{h}(\mathrm{T}_{k_j}),\, \Sigma_{\mathbf{w}}\right)}{\nu(\mathbf{z}_j \,|\, \mathbf{T})} \prod_{j:k_j = \emptyset} \frac{\nu_{cl}(\mathbf{z}_j \,|\, \mathbf{T})}{\nu(\mathbf{z}_j \,|\, \mathbf{T})} \end{aligned} \tag{19}$$

Substituting the log likelihood yields

$$\begin{aligned} Q\left(\mathrm{T} \,|\, \mathrm{T}^{(n)}\right) = &- \int_{\mathcal{T}} \nu(\mathbf{z} \,|\, \mathrm{T})\, d\mathbf{z} + \sum_{j=1}^{m} \sum_{k_1=1}^{N} \cdots \\ &\cdots \sum_{k_m=1}^{N} \log \mathcal{N}\left(\mathbf{z}_j \,|\, \mathbf{h}(\mathrm{T}_{k_j}),\, \Sigma_{\mathbf{w}}\right) \frac{\mathcal{N}\left(\mathbf{z}_j \,|\, \mathbf{h}\left(\mathrm{T}_{k_j}^{(n)}\right),\, \Sigma_{\mathbf{w}}\right)}{\nu\left(\mathbf{z}_j \,|\, \mathrm{T}^{(n)}\right)} \end{aligned} \tag{20}$$

Note that

$$\sum_{k_1,\cdots,k_{j-1},k_{j+1},\cdots,k_m=1}^{N} \log \mathcal{N}\left(\mathbf{z}_j \,|\, \mathbf{h}(\mathrm{T}_{k_j}),\, \Sigma_{\mathbf{w}}\right) \frac{\mathcal{N}\left(\mathbf{z}_j \,|\, \mathbf{h}\left(\mathrm{T}_{k_j}^{(n)}\right),\, \Sigma_{\mathbf{w}}\right)}{\nu\left(\mathbf{z}_j \,|\, \mathrm{T}^{(n)}\right)} = \log \mathcal{N}\left(\mathbf{z}_j \,|\, \mathbf{h}(\mathrm{T}_{k_j}),\, \Sigma_{\mathbf{w}}\right) \frac{\mathcal{N}\left(\mathbf{z}_j \,|\, \mathbf{h}\left(\mathrm{T}_{k_j}^{(n)}\right),\, \Sigma_{\mathbf{w}}\right)}{\nu\left(\mathbf{z}_j \,|\, \mathrm{T}^{(n)}\right)} \tag{21}$$

Thus, $Q\left(\mathrm{T} \,|\, \mathrm{T}^{(n)}\right)$ can be written as

$$Q\left(\mathrm{T} \,|\, \mathrm{T}^{(n)}\right) = \sum_{i=1}^{N} Q_i\left(\mathrm{T}_i \,|\, \mathrm{T}^{(n)}\right) \tag{22}$$

where

$$\begin{aligned} Q_i\left(\mathrm{T}_i \,|\, \mathrm{T}^{(n)}\right) = &- \int_{\mathcal{T}} \mathcal{N}\left(\mathbf{z} \,|\, \mathbf{h}(\mathrm{T}_i),\, \Sigma_{\mathbf{w}}\right) d\mathbf{z} \\ &+ \sum_{j=1}^{m} \frac{\mathcal{N}\left(\mathbf{z}_j \,|\, \mathbf{h}\left(\mathrm{T}_i^{(n)}\right),\, \Sigma_{\mathbf{w}}\right)}{\nu\left(\mathbf{z}_j \,|\, \mathrm{T}^{(n)}\right)} \log \mathcal{N}\left(\mathbf{z}_j \,|\, \mathbf{h}(\mathrm{T}_i),\, \Sigma_{\mathbf{w}}\right) \end{aligned} \tag{23}$$

This completes the E-step.

3.1.2 M - Step

The M-step maximizes $Q\left(\mathrm{T} \,|\, \mathrm{T}^{(n)}\right)$ over all feasible T, i.e.,

$$\mathrm{T}^{(n+1)} = \arg\max_{\mathrm{T}} \quad Q\left(\mathrm{T} \,|\, \mathrm{T}^{(n)}\right). \tag{24}$$

Assuming there is no functional relation between T_i and T_j for $i \neq j$, the required M-step maximum is found by maximizing the expressions $Q_i\left(\mathrm{T}_i \,|\, \mathrm{T}^{(n)}\right)$ separately. Let

$$\mathrm{T}_i^{(n+1)} = \arg\max_{\mathrm{T}_i} \quad Q_i\left(\mathrm{T}_i \,|\, \mathrm{T}^{(n)}\right), \qquad 1 \leq i \leq N. \tag{25}$$

Before we further proceed, note $\mathcal{N}\left(\mathbf{z}_j \,|\, \mathbf{h}(\mathrm{T}_i),\, \Sigma_{\mathbf{w}}\right)$ can be written as

$$\mathcal{N}\left(\mathbf{z}_j \,|\, \mathbf{h}(\mathrm{T}_i),\, \Sigma_{\mathbf{w}}\right) = \frac{1}{\sqrt{\det(2\pi\Sigma_{\mathbf{w}})}} \exp\left[-\frac{1}{2}\left(\mathbf{z}_j - \mathbf{h}(\mathrm{T}_i)\right)^T \Sigma_{\mathbf{w}}^{-1}\left(\mathbf{z}_j - \mathbf{h}(\mathrm{T}_i)\right)\right]. \tag{26}$$

Thus

$$\log \mathcal{N}\left(\mathbf{z}_j \mid \mathbf{h}(\mathrm{T}_i),\, \Sigma_{\mathbf{w}}\right) = -\log \sqrt{\det(2\pi\Sigma_{\mathbf{w}})} - \frac{1}{2}\left(\mathbf{z}_j - \mathbf{h}(\mathrm{T}_i)\right)^T \Sigma_{\mathbf{w}}^{-1}\left(\mathbf{z}_j - \mathbf{h}(\mathrm{T}_i)\right). \tag{27}$$

Define the weight $\omega_i\left(\mathbf{z}_j \mid \mathrm{T}^{(n)}, \Sigma_{\mathbf{w}}\right)$ as

$$\omega_i\left(\mathbf{z}_j \mid \mathrm{T}^{(n)}, \Sigma_{\mathbf{w}}\right) = \frac{\mathcal{N}\left(\mathbf{z}_j \mid \mathbf{h}\left(\mathrm{T}_i^{(n)}\right),\, \Sigma_{\mathbf{w}}\right)}{\nu\left(\mathbf{z}_j \mid \mathrm{T}^{(n)}\right)}. \tag{28}$$

The weight $\omega_i\left(\mathbf{z}_j \mid \mathrm{T}^{(n)}, \Sigma_{\mathbf{w}}\right)$ is the probability that the point $\mathbf{z}_j$ is generated by the i-th component given the current estimates $\mathrm{T}^{(n)}$. Now equation 25 can be rewritten as

$$\mathrm{T}_i^{(n+1)} = \arg\max_{\mathrm{T}_i} \quad -\int_{\mathcal{T}} \mathcal{N}\left(\mathbf{z} \mid \mathbf{h}(\mathrm{T}_i),\, \Sigma_{\mathbf{w}}\right) d\mathbf{z} + \sum_{j=1}^{m} \omega_i\left(\mathbf{z}_j \mid \mathrm{T}^{(n)}, \Sigma_{\mathbf{w}}\right) \log \mathcal{N}\left(\mathbf{z}_j \mid \mathbf{h}(\mathrm{T}_i),\, \Sigma_{\mathbf{w}}\right) \tag{29}$$

Then $\mathrm{T}_i^{(n+1)}$ satisfies the necessary condition:

$$\begin{aligned} &\sum_{j=1}^{m} \omega_i\left(\mathbf{z}_j \mid \mathrm{T}^{(n)}, \Sigma_{\mathbf{w}}\right) \Sigma_{\mathbf{w}}^{-1}\left[\mathbf{z}_j - \mathbf{h}(\mathrm{T}_i)\right] \nabla_{\mathrm{T}_i}\mathbf{h}\left(\mathrm{T}_i\right) = \\ &\int_{\mathcal{T}} \mathcal{N}\left(\mathbf{z} \mid \mathbf{h}(\mathrm{T}_i),\, \Sigma_{\mathbf{w}}\right) \Sigma_{\mathbf{w}}^{-1}\left[\mathbf{z} - \mathbf{h}(\mathrm{T}_i)\right] \nabla_{\mathrm{T}_i}\mathbf{h}\left(\mathrm{T}_i\right) d\mathbf{z} \end{aligned} \tag{30}$$

The above condition may be simplified to

$$\sum_{j=1}^{m} \omega_i\left(\mathbf{z}_j \mid \mathrm{T}^{(n)}, \Sigma_{\mathbf{w}}\right)\left[\mathbf{z}_j - \mathbf{h}(\mathrm{T}_i)\right] = \int_{\mathcal{T}} \mathcal{N}\left(\mathbf{z} \mid \mathbf{h}(\mathrm{T}_i),\, \Sigma_{\mathbf{w}}\right)\left[\mathbf{z} - \mathbf{h}(\mathrm{T}_i)\right] d\mathbf{z} \tag{31}$$

Based on the assumptions $\int_{\mathcal{T}} \mathcal{N}\left(\mathbf{z} \mid \mathbf{h}(\mathrm{T}_i),\, \Sigma_{\mathbf{w}}\right) \mathbf{z}\, d\mathbf{z} \approx \mathbf{h}(\mathrm{T}_i)$ and $\int_{\mathcal{T}} \mathcal{N}\left(\mathbf{z} \mid \mathbf{h}(\mathrm{T}_i),\, \Sigma_{\mathbf{w}}\right) d\mathbf{z} \approx 1$, the EM updates $\mathrm{T}_i^{(n+1)}$ is calculated as the solution to the equation

$$\mathbf{h}\left(\mathrm{T}_i^{n+1}\right) \approx \frac{\sum_{j=1}^{m} \omega_i\left(\mathbf{z}_j \mid \mathrm{T}^{(n)}, \Sigma_{\mathbf{w}}\right) \mathbf{z}_j}{\sum_{j=1}^{m} \omega_i\left(\mathbf{z}_j \mid \mathrm{T}^{(n)}, \Sigma_{\mathbf{w}}\right)}. \tag{32}$$

Define

$$\mathbf{y}_i = \begin{bmatrix} y_{r_i} \\ y_{\phi_i} \end{bmatrix} = \frac{\sum_{j=1}^{m} \omega_i \left(\mathbf{z}_j \,|\, \mathrm{T}^{(n)}, \Sigma_{\mathbf{w}} \right) \, \mathbf{z}_j}{\sum_{j=1}^{m} \omega_i \left(\mathbf{z}_j \,|\, \mathrm{T}^{(n)}, \Sigma_{\mathbf{w}} \right)}. \tag{33}$$

Now $\mathrm{T}_i^{(n+1)}$ is the solution to the nonlinear equation

$$\begin{bmatrix} \sqrt{(T_{x_i}^{(n+1)} - S_x)^2 + (T_{y_i}^{(n+1)} - S_y)^2} \\ \arctan((T_{x_i}^{(n+1)} - S_x)/(T_{y_i}^{(n+1)} - S_y)) \end{bmatrix} = \begin{bmatrix} y_{r_i} \\ y_{\phi_i} \end{bmatrix}. \tag{34}$$

Thus we have

$$T_{x_i}^{(n+1)} = \begin{cases} \left(\frac{y_{r_i}^2}{1+\tan^2\left(y_{\phi_i}\right)} \right)^{1/2} + S_x, & \text{if} \quad -\frac{\pi}{2} \le y_{\phi_i} \le \frac{\pi}{2}; \\ -\left(\frac{y_{r_i}^2}{1+\tan^2\left(y_{\phi_i}\right)} \right)^{1/2} + S_x, & \text{else,} \end{cases} \tag{35}$$

and

$$T_{y_i}^{(n+1)} = \tan\left(y_{\phi_i}\right) \left(T_{x_i}^{(n+1)} - S_x \right) + S_y. \tag{36}$$

Given the likelihood function is bounded above, the EM iteration nearly always converges to a local maximum of the likelihood function. However, the convergence rate is only linear and the first few iterations are commonly observed to result in significant improvements in the likelihood function.

3.2 Information Criteria for Model Selection

The previous subsection provides an approach to estimate the target locations given the number of targets. Presented in this section is an information theoretic approach to select the appropriate model, i.e., the number of targets or the number of Gaussian components. Model selection can be approached in terms of the Kullback-Leibler information of the true model with respect to the fitted model. Let $\nu(\mathbf{z} \,|\, \mathrm{T},\ N)$ be the true intensity and let $\nu(\mathbf{z} \,|\, \widehat{\mathrm{T}},\ \widehat{N})$ denote one of the fitted

models, i.e.,

$$\nu(\mathbf{z} \,|\, \mathrm{T},\, N) = \sum_{i=1}^{N} \mathcal{N}\left(\, \mathbf{z} \,|\, \mathbf{h}(\mathrm{T}_i),\, \Sigma_{\mathbf{w}} \,\right) \tag{37}$$

$$\nu(\mathbf{z} \,|\, \widehat{\mathrm{T}},\, \widehat{N}) = \sum_{i=1}^{\widehat{N}} \mathcal{N}\left(\mathbf{z} \,|\, \mathbf{h}(\widehat{\mathrm{T}}_i),\, \Sigma_{\mathbf{w}} \right). \tag{38}$$

Thus, the true distribution of $\mathbf{z}$ can be written as

$$p(\mathbf{z}) = \frac{1}{N} \sum_{i=1}^{N} \mathcal{N}\left(\, \mathbf{z} \,|\, \mathbf{h}(\mathrm{T}_i),\, \Sigma_{\mathbf{w}} \,\right), \tag{39}$$

and its approximation

$$\hat{p}(\mathbf{z}) = \frac{1}{\widehat{N}} \sum_{i=1}^{\widehat{N}} \mathcal{N}\left(\mathbf{z} \,|\, \mathbf{h}(\widehat{\mathrm{T}}_i),\, \Sigma_{\mathbf{w}} \right). \tag{40}$$

Now the Kullback-Leibler information of $p(\mathbf{z})$ with respect to $\hat{p}(\mathbf{z})$ is

$$D_{\mathrm{KL}}(p|\hat{p}) = \int_{\mathcal{T}} p(\mathbf{z}) \log p(\mathbf{z})\, d\mathbf{z} - \int_{\mathcal{T}} p(\mathbf{z}) \log \hat{p}(\mathbf{z})\, d\mathbf{z}, \tag{41}$$

which is a measure of the divergence of $p(\mathbf{z})$ relative to $\hat{p}(\mathbf{z})$. The aim is make the Kullback-Leibler information small. As the first term on the right-hand side of equation 41 does not depend on the model, only the second term is relevant. It can be expressed as

$$\eta(\{\mathbf{z}_1,\, \ldots,\, \mathbf{z}_m\} \,|P) = \int_{\mathcal{T}} \log \hat{p}(\mathbf{z})\, p(\mathbf{z}) d\mathbf{z}, \tag{42}$$

$$= \int_{\mathcal{T}} \log \hat{p}(\mathbf{z})\, dP(\mathbf{z}), \tag{43}$$

where P denotes the true distribution and $\{\mathbf{z}_1,\, \ldots,\, \mathbf{z}_m\}$ is the observed data. Now the sample estimate of $\eta(\{\mathbf{z}_1,\, \ldots,\, \mathbf{z}_m\} \,|P)$ is given by

$$\eta(\{\mathbf{z}_1,\, \ldots,\, \mathbf{z}_m\} \,|\widehat{P}) = \frac{1}{m} \sum_{j=1}^{m} \log \hat{p}(\mathbf{z}_j) \tag{44}$$

$$= \frac{1}{m} \log \mathfrak{L}\left(\{\mathbf{z}_1,\, \ldots,\, \mathbf{z}_m\} \,\middle|\, \widehat{\mathrm{T}},\, \widehat{N} \right), \tag{45}$$

where $\mathfrak{L}(\cdot)$ indicate the likelihood function and equation 45 follows from the assumption that the observations are independent. The bias of $\eta(\{\mathbf{z}_1,\, \ldots,\, \mathbf{z}_m\} \,|\widehat{P})$ as an estimator of

$\eta(\{\mathbf{z}_1, \ldots, \mathbf{z}_m\}|P)$ is the functional

$$b(P) = E_P\left[\eta(\{\mathbf{z}_1, \ldots, \mathbf{z}_m\}|\widehat{P}) - \eta(\{\mathbf{z}_1, \ldots, \mathbf{z}_m\}|P)\right], \tag{46}$$

where E_P denotes expectation with respect to the true distribution P. Thus, an information criterion for model section can be based on the bias-corrected log likelihood given by

$$\log \mathfrak{L}\left(\{\mathbf{z}_1, \ldots, \mathbf{z}_m\} \,\middle|\, \widehat{\mathrm{T}}, \widehat{N}\right) - b(P), \tag{47}$$

using an appropriate estimate of the bias term. The intent is to select the model that would maximize the above quantity and thus minimizes the Kullback-Leibler information. In the literature, the information criteria formed are generally expressed in terms of twice the negative value of the difference given above, so they are of the form

$$-2\log \mathfrak{L}\left(\{\mathbf{z}_1, \ldots, \mathbf{z}_m\} \,\middle|\, \widehat{\mathrm{T}}, \widehat{N}\right) + 2b(P), \tag{48}$$

The intent therefore is to choose a model to minimize the criterion equation 48.

3.2.1 Akaike's Information Criterion (AIC)

Akaike (*29*) showed that $b(P)$ is asymptotically equal to d, where d is equal to the total number of parameters in the model. Thus from equation 48, AIC selects the model that minimizes

$$-2\log \mathfrak{L}\left(\{\mathbf{z}_1, \ldots, \mathbf{z}_m\} \,\middle|\, \widehat{\mathrm{T}}, \widehat{N}\right) + 2d. \tag{49}$$

For the 2-D localization problem under consideration, the above criterion can be rewritten as

$$-2\log \mathfrak{L}\left(\{\mathbf{z}_1, \ldots, \mathbf{z}_m\} \,\middle|\, \widehat{\mathrm{T}}, \widehat{N}\right) + 4\widehat{N}. \tag{50}$$

Therefore, the present approach would select several different candidates for $\widehat{N}$ and solve the corresponding localization problem using the EM algorithm. Afterwards, the AIC associated with each model is calculated and the model corresponding to the lowest AIC is selected as the estimated model. A summary of the proposed algorithm is presented in table 1.

Table 1. Summary of algorithm.

Given data: $\{\mathbf{z}_1, \ldots, \mathbf{z}_m\}$

Fit the intensity: $\nu(\mathbf{z} \,|\, \mathrm{T},\, N) = \sum_{i=1}^{N} \mathcal{N}\,(\,\mathbf{z} \,|\, \mathbf{h}(\mathrm{T}_i),\, \Sigma_{\mathbf{w}}\,)$

Estimate the parameters: N and $\{\mathrm{T}_1, \ldots, \mathrm{T}_N\}$

- *Select the candidate models*: $\widehat{N}_1, \ldots, \widehat{N}_K$
- FOR $k = 1 : K$
  - FOR $i = 1 : \widehat{N}_k$
    - *Initialize* $\mathrm{T}_i^{(0)}(k) \in \mathcal{T}$
  - END FOR
  - FOR *EM iteration* $n = 0, 1, \ldots$ *until converges*
    - FOR $i = 1 : \widehat{N}_k$
      - *Update* $T_{x_i}^{(n+1)}(k)$ *using equation 35*
      - *Update* $T_{y_i}^{(n+1)}(k)$ *using equation 36*
    - END FOR
  - END FOR
  - *Calculate the maximum likelihood:* $\mathfrak{L}_k = \exp\{-\widehat{N}_k\} \prod_{j=1}^{m} \nu(\mathbf{z}_j \,|\, \widehat{\mathrm{T}}(k),\, \widehat{N}_k)$
  - *Calculate* $AIC(k) = -2 \log \mathfrak{L}_k + 4\widehat{N}_k$
- END FOR
- *Select the index* k *corresponding to the minimum AIC:*

$$\jmath = \min_k \{AIC(1), \ldots, AIC(k), \ldots, AIC(K)\}$$

- *Parameter estimates are* $\widehat{N}_\jmath$ *and* $\widehat{\mathrm{T}}(\jmath)$

4. Numerical Example

Consider a scenario, where there are four targets ($N = 4$) located at

$$\mathrm{T} = \left(\begin{bmatrix} 298 \\ -5 \end{bmatrix}, \begin{bmatrix} 250 \\ 7 \end{bmatrix}, \begin{bmatrix} 267 \\ -17 \end{bmatrix}, \begin{bmatrix} 310 \\ 18 \end{bmatrix} \right).$$

Following the setup presented in section 2., the measurement intensity is given as

$$\nu(\mathbf{z} \,|\, \mathbf{T}) = \sum_{i=1}^{4} I_i \mathcal{N}\left(\mathbf{z} \,|\, \mathbf{h}(\mathrm{T}_i),\, \Sigma_{\mathbf{w}} \right) + \nu_{cl}(\mathbf{z}),$$

where the known measurement covariance matrix is $\Sigma_{\mathbf{w}} = \begin{bmatrix} 9 & 0 \\ 0 & 5 \times 10^{-3} \end{bmatrix}$, i.e., the range standard deviation amounts to 3 m and the bearing standard deviation to 4^o. The I_i's are given as

$$I_{1:4} = \{0.5732, 1.7962, 1.2172, 0.4135\}$$

and the clutter intensity is given as

$$\nu_{cl}(\mathbf{z}) = 0.0122 \mathcal{N}\left(\mathbf{z} \,|\, \mathbf{h}\left(\begin{bmatrix} 281.25 \\ 0.75 \end{bmatrix} \right), \begin{bmatrix} 900 & 0 \\ 0 & 0.4874 \end{bmatrix} \right).$$

The sensor location is selected as $S_x = 10$ and $S_y = 0$. In order to evaluate the performance of the algorithm, 200 MC runs were conducted. For each run, the number of measurements are determined by sampling from the Poisson distribution:

$$p_M(m) \approx \frac{(4)^m}{m!} \exp\{-4\}.$$

The m measurements are obtained from the mixture pdf:

$$\frac{1}{4.0122} \left[\sum_{i=1}^{4} I_i \mathcal{N}\left(\mathbf{z} \,|\, \mathbf{h}(\mathrm{T}_i),\, \Sigma_{\mathbf{w}} \right) + 0.0122 \mathcal{N}\left(\mathbf{z} \,|\, \mathbf{h}\left(\begin{bmatrix} 281.25 \\ 0.75 \end{bmatrix} \right), \begin{bmatrix} 900 & 0 \\ 0 & 0.4874 \end{bmatrix} \right) \right] \quad (51)$$

with mixing probabilities $\{0.1429, 0.4477, 0.3034, 0.1031, 0.0030\}$. Here we use the optimal subpattern assignment (OSPA) metric to assess the performance of the localization algorithm (*30*). To be specific, we use the OSPA metric of order 1 with cut-off value 100.

Given in figure 1 is the histogram obtained from the MC runs for the number of measurements and estimated number of targets. Note that the histogram for the number of measurements clearly resembles that of a Poisson pdf while the histogram for the estimated number of targets clearly favors 4.

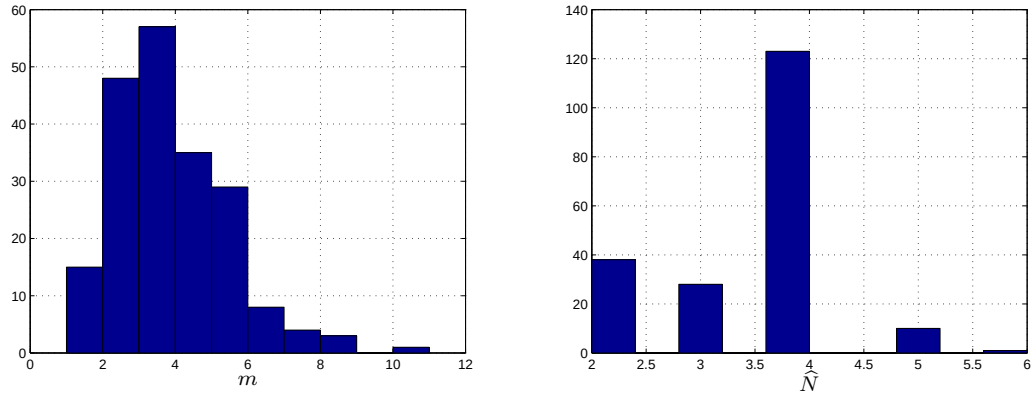

(a) Number of measurements (b) Estimated number of targets

Figure 1. Histogram for number of measurements and estimated number of targets.

Figure 2 contains the OSPA metric obtained for each MC runs. Note that the OSPA metric around the 100 mark indicates the MC runs with a cardinality error of one while the OSPA metric around the 200 mark indicates the MC runs with a cardinality error of two. Note that the majority of the metrics are well below 25 indicating no cardinality error and accurate localization.

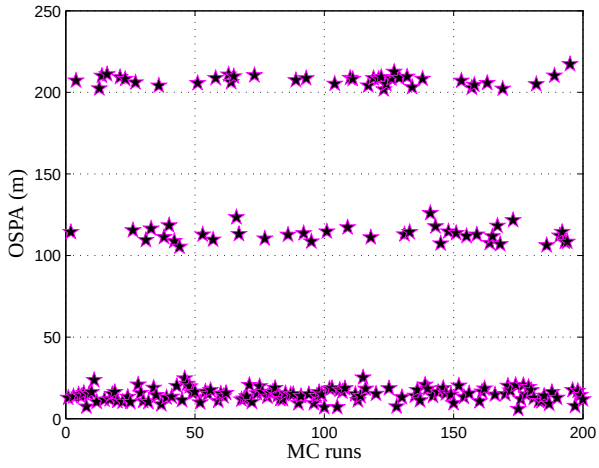

Figure 2. OSPA metric for each MC runs.

Given in figure 3 is the localization results obtained for one of the MC trials. For the numerical

results presented in figure 3, $m = 7$ and the measurement are

$$\mathbf{z} = \left(\begin{bmatrix} 295.4439 \\ -7.4361 \end{bmatrix}, \begin{bmatrix} 248.0845 \\ 7.9683 \end{bmatrix}, \begin{bmatrix} 266.9659 \\ -19.7274 \end{bmatrix}, \begin{bmatrix} 308.8356 \\ 17.9654 \end{bmatrix}, \begin{bmatrix} 301.3977 \\ -2.3297 \end{bmatrix}, \begin{bmatrix} 251.7503 \\ 6.9274 \end{bmatrix}, \begin{bmatrix} 251.5474 \\ 3.2172 \end{bmatrix} \right).$$

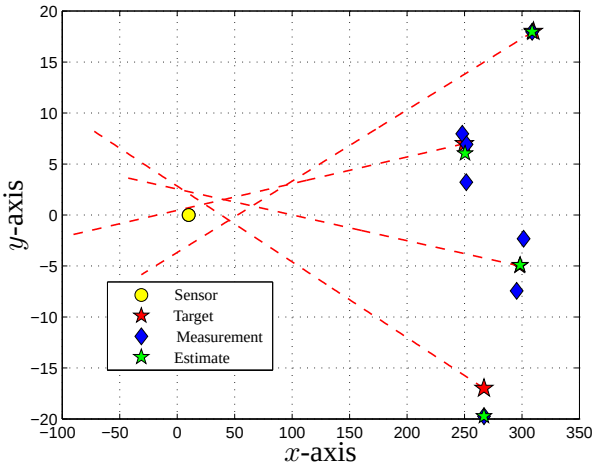

Figure 3. Single-sensor simulation scenario.

For all MC runs, five different models are selected and their corresponding AIC are given in table 2.

Table 2. Models and AIC.

AIC				
$\widehat{N}_1 = 2$	$\widehat{N}_1 = 3$	$\widehat{N}_1 = 4$	$\widehat{N}_1 = 5$	$\widehat{N}_1 = 6$
26.7675	24.7321	24.3130	27.1980	31.8099

Thus, the parameter estimates are $\widehat{N} = 4$ and

$$\widehat{\mathrm{T}} = \left(\begin{bmatrix} 298.4321 \\ -4.9096 \end{bmatrix}, \begin{bmatrix} 250.4694 \\ 6.0468 \end{bmatrix}, \begin{bmatrix} 266.9659 \\ -19.7274 \end{bmatrix}, \begin{bmatrix} 308.8356 \\ 17.9654 \end{bmatrix} \right).$$

5. Multi-Sensor Problem Formulation

This section considers a multi-sensor scenario where there are 's' sensors located at points

$$(S_1,\, S_2,\, \ldots,\, S_s) = \left(\begin{bmatrix} S_{x_1} \\ S_{y_1} \end{bmatrix},\, \begin{bmatrix} S_{x_2} \\ S_{y_2} \end{bmatrix},\, \ldots,\, \begin{bmatrix} S_{x_s} \\ S_{y_s} \end{bmatrix} \right). \tag{52}$$

The sensor locations are known a priori. Following the problem formulation given in section 2., the number of measurements and the measurement set are jointly modeled as a PPP. Thus, consider the s different realizations of s PPPs, $\mathbf{\Psi}^{(1)}, \mathbf{\Psi}^{(2)}, \ldots, \mathbf{\Psi}^{(s)}$:

$$\begin{aligned} \boldsymbol{\psi}^{(1)} &= \left(m_1, \left\{ \mathbf{z}_1^{(1)},\, \mathbf{z}_2^{(1)},\, \ldots,\, \mathbf{z}_{m_1}^{(1)} \right\} \right), \\ &\vdots \qquad\qquad\qquad\qquad \vdots \\ \boldsymbol{\psi}^{(\ell)} &= \left(m_\ell, \left\{ \mathbf{z}_1^{(\ell)},\, \mathbf{z}_2^{(\ell)},\, \ldots,\, \mathbf{z}_{m_\ell}^{(\ell)} \right\} \right), \\ &\vdots \qquad\qquad\qquad\qquad \vdots \\ \boldsymbol{\psi}^{(s)} &= \left(m_s, \left\{ \mathbf{z}_1^{(s)},\, \mathbf{z}_2^{(s)},\, \ldots,\, \mathbf{z}_{m_s}^{(s)} \right\} \right). \end{aligned}$$

For $\ell = 1, \ldots, s$, the ℓ-th realization, i.e., $\boldsymbol{\psi}^{(\ell)}$, corresponds to the number of measurements and the measurement set obtained by the ℓ-th sensor. The measurement noise is assumed to be zero-mean Gaussian with known variance $\Sigma_{\mathbf{w}}$. Now following the similar formulation presented for the single-sensor scenario, the ℓ-th PPP is modeled via the intensity function

$$\nu^{(\ell)}(\mathbf{z}) = \sum_{i=1}^{N} p^D(\mathrm{T}_i)\, \mathcal{N}\left(\mathbf{z} | \mathbf{h}\left(\mathrm{T}_i, S_\ell\right), \Sigma_{\mathbf{w}}\right) + \nu_{cl}^{(\ell)}(\mathbf{z}).$$

Let $\boldsymbol{\psi}_{1:s}$ denotes the set of all measurements, i.e.,

$$\boldsymbol{\psi}_{1:s} = \left(\sum_{\ell=1}^{s} m_\ell,\, \left\{ \mathbf{z}_1^{(1)},\, \ldots,\, \mathbf{z}_{m_1}^{(1)}, \ldots, \mathbf{z}_1^{(\ell)},\, \ldots,\, \mathbf{z}_{m_\ell}^{(\ell)}, \ldots, \mathbf{z}_1^{(s)},\, \ldots,\, \mathbf{z}_{m_s}^{(s)} \right\} \right).$$

Since the superposition of two PPPs is also a PPP, $\boldsymbol{\psi}_{1:s}$ can be considered as a PPP with intensity

$$\gamma(\mathbf{z}) = \sum_{\ell=1}^{s} \nu^{(\ell)}(\mathbf{z}) = \sum_{\ell=1}^{s} \left(\sum_{i=1}^{N} p^D(\mathrm{T}_i)\, \mathcal{N}\left(\mathbf{z} | \mathbf{h}\left(\mathrm{T}_i, S_\ell\right), \Sigma_{\mathbf{w}}\right) + \nu_{cl}^{(\ell)}(\mathbf{z}) \right).$$

Now $p\left(\boldsymbol{\psi}_{1:s}\right)$ can be written as

$$p\left(\boldsymbol{\psi}_{1:s}\right) = \exp\left\{-\int_{\mathcal{T}} \gamma(\mathbf{z})\, d\mathbf{z}\right\} \prod_{\ell=1}^{s} \prod_{j=1}^{m_\ell} \gamma(\mathbf{z}_j^{(\ell)}). \tag{53}$$

6. Multi-Sensor Solution

The multi-sensor solution proposed in this section directly follows from the single-sensor solution presented previously.

6.1 EM Method

Given the number of targets, N, the intensity $\nu^{(\ell)}(\mathbf{z} \mid \mathbf{T})$ of the ℓ-th sensor is the superposition of N Gaussian components along with the clutter intensities:

$$\nu^{(\ell)}(\mathbf{z} \mid \mathbf{T}) = \sum_{i=1}^{N} p^D(\mathrm{T}_i)\, \mathcal{N}\left(\mathbf{z} | \mathbf{h}\left(\mathrm{T}_i, S_\ell\right), \Sigma_{\mathbf{w}}\right) + \nu_{cl}^{(\ell)}(\mathbf{z}). \tag{54}$$

6.1.1 E - Step

First consider the ℓ-th sensor, where there are m_ℓ measurements. For $j = 1, \ldots, m_\ell$, the natural choice of the "missing data" for the ℓ-th PPP are the conditionally independent random indices $k_j^{(\ell)}$, $k_j^{(\ell)} \in \{\emptyset, 1, 2, \ldots, N\}$, that identify which of the Gaussian components, i.e., target, generated the measurement $\mathbf{z}_j^{(\ell)}$. Here $k_j = \emptyset$ indicates that the measurement is generated by clutter. Let

$$\mathbf{z}_c^{(\ell)} = \left(m_\ell\,,\, \{(\mathbf{z}_1^{(\ell)}, k_1^{(\ell)}), \ldots, (\mathbf{z}_j^{(\ell)}, k_j^{(\ell)}), \ldots, (\mathbf{z}_{m_\ell}^{(\ell)}, k_{m_\ell}^{(\ell)})\}\right) \tag{55}$$

denote the complete data. For $i \in \{\emptyset, 1, 2, \ldots, N\}$, let

$$\mathbf{z}_c^{(\ell)}(i) = \{(\mathbf{z}_j^{(\ell)}, k_j^{(\ell)}) \,:\, k_j^{(\ell)} = i\}. \tag{56}$$

Let $n_c^{(\ell)}(i) \geq 0$ denote the number of indices j such that $k_j^{(\ell)} = i$, and let

$$\psi_c^{(\ell)}(i) = \left(\, n_c^{(\ell)}(i),\, \mathbf{z}_c^{(\ell)}(i)\,\right). \tag{57}$$

It follows from the definition of $k_j^{(\ell)}$ that $\psi_c^{(\ell)}(i)$ is a realization of the PPP whose intensity is

$$\psi_c^{(\ell)}(i) \sim \begin{cases} p^D(\mathrm{T}_i)\,\mathcal{N}\left(\mathbf{z}|\mathbf{h}\left(\mathrm{T}_i, S_\ell\right), \Sigma_{\mathbf{w}}\right), & \text{if } i \in \{1, 2, \ldots, N\}; \\ \nu_{cl}^{(\ell)}(\mathbf{z}), & \text{if } i = \emptyset. \end{cases} \tag{58}$$

Now only considering the first scenario, $i \in \{1, 2, \ldots, N\}$, the pdf of $\psi_c^{(\ell)}(i)$ can be written as

$$\begin{aligned} p\left(\psi_c^{(\ell)}(i) \mid \mathbf{T}\right) = &\exp\left(-\int_{\mathcal{T}} p^D(\mathrm{T}_i)\,\mathcal{N}\left(\mathbf{z}|\mathbf{h}\left(\mathrm{T}_i, S_\ell\right), \Sigma_{\mathbf{w}}\right) d\mathbf{z}\right) \\ &\prod_{j:k_j^{(\ell)}=i} p^D(\mathrm{T}_i)\,\mathcal{N}\left(\mathbf{z}_j^{(\ell)}|\mathbf{h}\left(\mathrm{T}_i, S_\ell\right), \Sigma_{\mathbf{w}}\right) \end{aligned} \tag{59}$$

and

$$p\left(\psi_c^{(\ell)}(\emptyset) \mid \mathbf{T}\right) = \exp\left(-\int_{\mathcal{T}} \nu_{cl}^{(\ell)}(\mathbf{z})\, d\mathbf{z}\right) \prod_{j:k_j^{(\ell)}=\emptyset} \nu_{cl}^{(\ell)}(\mathbf{z}_j^{(\ell)}) \tag{60}$$

Since the superposed components are independent, we have

$$\begin{aligned} &p\left(\mathbf{z}_c^{(\ell)} \mid \mathbf{T}\right) = p\left(\psi_c^{(\ell)}(\emptyset) \mid \mathbf{T}\right) p\left(\psi_c^{(\ell)}(1) \mid \mathbf{T}\right) p\left(\psi_c^{(\ell)}(2) \mid \mathbf{T}\right) \ldots p\left(\psi_c^{(\ell)}(N) \mid \mathbf{T}\right) \\ &= \exp\left(-\int_{\mathcal{T}} \nu^{(\ell)}(\mathbf{z} \mid \mathbf{T})\, d\mathbf{z}\right) \prod_{j:k_j^{(\ell)}\neq\emptyset} p^D(\mathrm{T}_{k_j^{(\ell)}})\,\mathcal{N}\left(\mathbf{z}_j^{(\ell)} \mid \mathbf{h}(\mathrm{T}_{k_j^{(\ell)}}, S_\ell),\, \Sigma_{\mathbf{w}}\right) \prod_{j:k_j^{(\ell)}=\emptyset} \nu_{cl}^{(\ell)}(\mathbf{z}_j^{(\ell)}) \end{aligned}$$

Let

$$\mu^{(\ell)}\left(\mathbf{z}_j^{(\ell)} \mid \mathrm{T}_{k_j^{(\ell)}}\right) = \begin{cases} p^D(\mathrm{T}_{k_j^{(\ell)}})\,\mathcal{N}\left(\mathbf{z}_j^{(\ell)} \mid \mathbf{h}(\mathrm{T}_{k_j^{(\ell)}}, S_\ell),\, \Sigma_{\mathbf{w}}\right), & \text{if } k_j^{(\ell)} \in \{1, 2, \ldots, N\}; \\ \nu_{cl}^{(\ell)}(\mathbf{z}_j^{(\ell)}), & \text{if } k_j^{(\ell)} = \emptyset. \end{cases} \tag{61}$$

Then

$$p\left(\mathbf{z}_c^{(\ell)} \mid \mathbf{T}\right) = \exp\left(-\int_{\mathcal{T}} \nu^{(\ell)}(\mathbf{z} \mid \mathbf{T})\, d\mathbf{z}\right) \prod_{j=1}^{m_\ell} \mu^{(\ell)}\left(\mathbf{z}_j^{(\ell)} \mid \mathrm{T}_{k_j^{(\ell)}}\right) \tag{62}$$

The log likelihood function of $\mathbf{T}$ given $\mathbf{z}_c^{(\ell)}$ is

$$\mathfrak{L}\left(\mathbf{T} \mid \mathbf{z}_c^{(\ell)}\right) = -\int_{\mathcal{T}} \nu^{(\ell)}(\mathbf{z} \mid \mathbf{T})\, d\mathbf{z} + \sum_{j=1}^{m_\ell} \log\, \mu^{(\ell)}\left(\mathbf{z}_j^{(\ell)} \mid \mathrm{T}_{k_j^{(\ell)}}\right) \tag{63}$$

Now note that

$$p\left(\boldsymbol{\psi}^{(\ell)} \mid \mathbf{T}\right) = \exp\left(-\int_{\mathcal{T}} \nu^{(\ell)}(\mathbf{z} \mid \mathbf{T})\, d\mathbf{z}\right) \prod_{j=1}^{m_\ell} \nu^{(\ell)}\left(\mathbf{z}_j^{(\ell)} \mid \mathbf{T}\right) \tag{64}$$

Thus the conditional pdf of the missing data, $\left(k_1^{(\ell)}, \ldots, k_m^{(\ell)}\right)$, can be written as

$$p\left(k_1^{(\ell)}, \ldots, k_{m_\ell}^{(\ell)} \mid \boldsymbol{\psi}^{(\ell)}, \mathbf{T}\right) = \frac{p\left(\mathbf{z}_c^{(\ell)} \mid \mathbf{T}\right)}{p\left(\boldsymbol{\psi}^{(\ell)} \mid \mathbf{T}\right)} = \prod_{j=1}^{m_\ell} \frac{\mu^{(\ell)}\left(\mathbf{z}_j^{(\ell)} \mid \mathrm{T}_{k_j^{(\ell)}}\right)}{\nu^{(\ell)}\left(\mathbf{z}_j^{(\ell)} \mid \mathbf{T}\right)} \tag{65}$$

Furthermore, assuming that the sensor measurements conditioned on the target locations are independent of each other yields

$$p\left(\mathbf{z}_c^{(1)}, \ldots, \mathbf{z}_c^{(s)} \mid \mathbf{T}\right) = p\left(\mathbf{z}_c^{(1)} \mid \mathbf{T}\right) \ldots p\left(\mathbf{z}_c^{(s)} \mid \mathbf{T}\right) \tag{66}$$

$$= \prod_{\ell=1}^{s} \left[\exp\left(-\int_{\mathcal{T}} \nu^{(\ell)}(\mathbf{z} \mid \mathbf{T})\, d\mathbf{z}\right) \prod_{j=1}^{m_\ell} \mu^{(\ell)}\left(\mathbf{z}_j^{(\ell)} \mid \mathrm{T}_{k_j^{(\ell)}}\right)\right] \tag{67}$$

and

$$p\left(\boldsymbol{\psi}^{(1)}, \ldots, \boldsymbol{\psi}^{(s)} \mid \mathbf{T}\right) = p\left(\boldsymbol{\psi}^{(1)} \mid \mathbf{T}\right) \ldots p\left(\boldsymbol{\psi}^{(s)} \mid \mathbf{T}\right) \tag{68}$$

$$= \prod_{\ell=1}^{s} \left[\exp\left(-\int_{\mathcal{T}} \nu^{(\ell)}(\mathbf{z} \mid \mathbf{T})\, d\mathbf{z}\right) \prod_{j=1}^{m_\ell} \nu^{(\ell)}\left(\mathbf{z}_j^{(\ell)} \mid \mathbf{T}\right)\right] \tag{69}$$

Now the conditional pdf of the missing data for all sensors, $\left(k_1^{(1)}, \ldots, k_{m_1}^{(1)}, \ldots, k_1^{(s)}, \ldots, k_{m_s}^{(s)}\right)$, given $\mathbf{T}$ and $\boldsymbol{\psi}^{(1)}, \ldots, \boldsymbol{\psi}^{(s)}$ can be written as

$$p\left(k_1^{(1)}, \ldots, k_{m_s}^{(s)} \mid \boldsymbol{\psi}^{(1)}, \ldots, \boldsymbol{\psi}^{(s)}, \mathbf{T}\right) = \frac{p\left(\mathbf{z}_c^{(1)}, \ldots, \mathbf{z}_c^{(s)} \mid \mathbf{T}\right)}{p\left(\boldsymbol{\psi}^{(1)}, \ldots, \boldsymbol{\psi}^{(s)} \mid \mathbf{T}\right)} \tag{70}$$

$$= \prod_{\ell=1}^{s} \prod_{j=1}^{m_\ell} \frac{\mu^{(\ell)}\left(\mathbf{z}_j^{(\ell)} \mid \mathrm{T}_{k_j^{(\ell)}}\right)}{\nu^{(\ell)}\left(\mathbf{z}_j^{(\ell)} \mid \mathbf{T}\right)} \tag{71}$$

The log likelihood function of $\mathbf{T}$ given $\mathbf{z}_c^{(1)}, \ldots, \mathbf{z}_c^{(s)}$ is

$$\mathfrak{L}\left(\mathbf{T} \mid \mathbf{z}_c^{(1)}, \ldots, \mathbf{z}_c^{(s)}\right) = \sum_{\ell=1}^{s} \left[-\int_{\mathcal{T}} \nu^{(\ell)}(\mathbf{z} \mid \mathbf{T})\, d\mathbf{z} + \sum_{j=1}^{m_\ell} \log\, \mu^{(\ell)}\left(\mathbf{z}_j^{(\ell)} \mid \mathrm{T}_{k_j^{(\ell)}}\right)\right] \tag{72}$$

Given $\gamma(\mathbf{z} \,|\, \mathbf{T}) = \sum_{\ell=1}^{s} \nu^{(\ell)}(\mathbf{z} \,|\, \mathbf{T})$, the log likelihood function can be rewritten as

$$\mathfrak{L}\left(\mathbf{T} \,|\, \mathbf{z}_c^{(1)}, \ldots, \mathbf{z}_c^{(s)}\right) = -\int_{\mathcal{T}} \gamma(\mathbf{z} \,|\, \mathbf{T})\, d\mathbf{z} + \sum_{\ell=1}^{s} \sum_{j=1}^{m_\ell} \log\, \mu^{(\ell)}\left(\mathbf{z}_j^{(\ell)} \,|\, \mathrm{T}_{k_j^{(\ell)}}\right) \tag{73}$$

Let $n = 0, 1, \ldots$ denote the EM iteration index, and let the current feasible value of $\mathbf{T}$ be $\mathbf{T}^{(n)} = \left(\mathrm{T}_1^{(n)}, \ldots, \mathrm{T}_N^{(n)}\right)$. Now the EM auxiliary function is the conditional expectation

$$\begin{aligned} Q\left(\mathbf{T} \,\middle|\, \mathbf{T}^{(n)}\right) &= \mathbb{E}_{\mathbf{z}_c^{(1)}, \ldots, \mathbf{z}_c^{(s)} \,|\, \boldsymbol{\psi}^{(1)}, \ldots, \boldsymbol{\psi}^{(s)}, \mathbf{T}^{(n)}} \left[\mathfrak{L}\left(\mathbf{T} \,|\, \mathbf{z}_c^{(1)}, \ldots, \mathbf{z}_c^{(s)}\right) \,\middle|\, \boldsymbol{\psi}^{(1)}, \ldots, \boldsymbol{\psi}^{(s)}, \mathbf{T}^{(n)}\right] \\ &= \sum_{k_1^{(1)}=\emptyset}^{N} \cdots \sum_{k_{m_s}^{(s)}=\emptyset}^{N} \mathfrak{L}\left(\mathbf{T} \,|\, \mathbf{z}_c^{(1)}, \ldots, \mathbf{z}_c^{(s)}\right) \prod_{\alpha=1}^{s} \prod_{\beta=1}^{m_\alpha} \frac{\mu^{(\alpha)}\left(\mathbf{z}_\beta^{(\alpha)} \,|\, \mathrm{T}_{k_\beta^{(\alpha)}}^{(n)}\right)}{\nu^{(\alpha)}\left(\mathbf{z}_\beta^{(\alpha)} \,|\, \mathbf{T}^{(n)}\right)} \end{aligned} \tag{74}$$

Substituting the log likelihood yields

$$\begin{aligned} Q\left(\mathbf{T} \,|\, \mathbf{T}^{(n)}\right) &= -\int_{\mathcal{T}} \gamma(\mathbf{z} \,|\, \mathbf{T})\, d\mathbf{z} + \\ &\sum_{k_1^{(1)}=\emptyset}^{N} \cdots \sum_{k_{m_s}^{(s)}=\emptyset}^{N} \left[\sum_{\ell=1}^{s} \sum_{j=1}^{m_\ell} \log\, \mu^{(\ell)}\left(\mathbf{z}_j^{(\ell)} \,|\, \mathrm{T}_{k_j^{(\ell)}}\right)\right] \prod_{\alpha=1}^{s} \prod_{\beta=1}^{m_\alpha} \frac{\mu^{(\alpha)}\left(\mathbf{z}_\beta^{(\alpha)} \,|\, \mathrm{T}_{k_\beta^{(\alpha)}}^{(n)}\right)}{\nu^{(\alpha)}\left(\mathbf{z}_\beta^{(\alpha)} \,|\, \mathbf{T}^{(n)}\right)} \end{aligned} \tag{75}$$

Thus

$$\begin{aligned} Q\left(\mathbf{T} \,|\, \mathbf{T}^{(n)}\right) = \sum_{\ell=1}^{s} \sum_{j=1}^{m_\ell} \sum_{k_j^{(\ell)}=\emptyset}^{N} & \sum_{k_1^{(1)}, \cdots, k_{j-1}^{(\ell)}, k_{j+1}^{(\ell)}, \cdots, k_{m_s}^{(s)}=\emptyset}^{N} \log\, \mu^{(\ell)}\left(\mathbf{z}_j^{(\ell)} \,|\, \mathrm{T}_{k_j^{(\ell)}}\right) \\ & \times \prod_{\alpha=1}^{s} \prod_{\beta=1}^{m_\alpha} \frac{\mu^{(\alpha)}\left(\mathbf{z}_\beta^{(\alpha)} \,|\, \mathrm{T}_{k_\beta^{(\alpha)}}^{(n)}\right)}{\nu^{(\alpha)}\left(\mathbf{z}_\beta^{(\alpha)} \,|\, \mathbf{T}^{(n)}\right)} - \int_{\mathcal{T}} \gamma(\mathbf{z} \,|\, \mathbf{T})\, d\mathbf{z} \end{aligned} \tag{76}$$

Note

$$\sum_{k_1^{(1)}=\emptyset}^{N} \cdots \sum_{k_{m_s}^{(s)}=\emptyset}^{N} \left[\prod_{\ell=1}^{s} \prod_{j=1}^{m_\ell} \frac{\mu^{(\ell)}\left(\mathbf{z}_j^{(\ell)} \,|\, \mathrm{T}_{k_j^{(\ell)}}\right)}{\nu^{(\ell)}\left(\mathbf{z}_j^{(\ell)} \,|\, \mathbf{T}\right)}\right] = 1 \tag{77}$$

Thus we have

$$Q\left(\mathbf{T} \mid \mathbf{T}^{(n)}\right) = \sum_{\ell=1}^{s} \sum_{j=1}^{m_\ell} \sum_{k_j^{(\ell)}=\emptyset}^{N} \sum_{k_1^{(1)},\cdots,k_{j-1}^{(\ell)},k_{j+1}^{(\ell)},\cdots,k_{m_s}^{(s)}=\emptyset}^{N} \log\, \mu^{(\ell)}\left(\mathbf{z}_j^{(\ell)} \mid \mathrm{T}_{k_j^{(\ell)}}\right) \times \frac{\mu^{(\ell)}\left(\mathbf{z}_j^{(\ell)} \mid \mathrm{T}_{k_j^{(\ell)}}^{(n)}\right)}{\nu^{(\ell)}\left(\mathbf{z}_j^{(\ell)} \mid \mathbf{T}^{(n)}\right)} - \int_{\mathcal{T}} \gamma(\mathbf{z} \mid \mathrm{T})\, d\mathbf{z} \tag{78}$$

Note that

$$\sum_{k_1^{(1)},\cdots,k_{j-1}^{(\ell)},k_{j+1}^{(\ell)},\cdots,k_{m_s}^{(s)}=\emptyset}^{N} \log\, \mu^{(\ell)}\left(\mathbf{z}_j^{(\ell)} \mid \mathrm{T}_{k_j^{(\ell)}}\right) \frac{\mu^{(\ell)}\left(\mathbf{z}_j^{(\ell)} \mid \mathrm{T}_{k_j^{(\ell)}}^{(n)}\right)}{\nu^{(\ell)}\left(\mathbf{z}_j^{(\ell)} \mid \mathbf{T}^{(n)}\right)} = \log\, \mu^{(\ell)}\left(\mathbf{z}_j^{(\ell)} \mid \mathrm{T}_{k_j^{(\ell)}}\right) \frac{\mu^{(\ell)}\left(\mathbf{z}_j^{(\ell)} \mid \mathrm{T}_{k_j^{(\ell)}}^{(n)}\right)}{\nu^{(\ell)}\left(\mathbf{z}_j^{(\ell)} \mid \mathbf{T}^{(n)}\right)} \tag{79}$$

Thus, $Q\left(\mathbf{T} \mid \mathbf{T}^{(n)}\right)$ can be written as

$$Q\left(\mathbf{T} \mid \mathbf{T}^{(n)}\right) = \sum_{i=\emptyset}^{N} \sum_{\ell=1}^{s} \sum_{j=1}^{m_\ell} \log\, \mu^{(\ell)}\left(\mathbf{z}_j^{(\ell)} \mid \mathrm{T}_i\right) \frac{\mu^{(\ell)}\left(\mathbf{z}_j^{(\ell)} \mid \mathrm{T}_i^{(n)}\right)}{\nu^{(\ell)}\left(\mathbf{z}_j^{(\ell)} \mid \mathbf{T}^{(n)}\right)} - \int_{\mathcal{T}} \gamma(\mathbf{z} \mid \mathrm{T})\, d\mathbf{z} \tag{80}$$

Now substituting equation 61, $Q\left(\mathbf{T} \mid \mathbf{T}^{(n)}\right)$ can be rewritten as

$$Q\left(\mathbf{T} \mid \mathbf{T}^{(n)}\right) = -\int_{\mathcal{T}} \gamma(\mathbf{z} \mid \mathrm{T})\, d\mathbf{z} + \sum_{\ell=1}^{s} \sum_{j=1}^{m_\ell} \log\, \nu_{cl}^{(\ell)}(\mathbf{z}_j^{(\ell)}) \frac{\nu_{cl}^{(\ell)}(\mathbf{z}_j^{(\ell)})}{\nu^{(\ell)}\left(\mathbf{z}_j^{(\ell)} \mid \mathbf{T}^{(n)}\right)} + \sum_{i=1}^{N} \sum_{\ell=1}^{s} \sum_{j=1}^{m_\ell} \log\, p^D(\mathrm{T}_i)\, \mathcal{N}\left(\mathbf{z}_j^{(\ell)} \mid \mathbf{h}(\mathrm{T}_i, S_\ell),\, \Sigma_{\mathbf{w}}\right) \frac{p^D(\mathrm{T}_i^{(n)})\, \mathcal{N}\left(\mathbf{z}_j^{(\ell)} \mid \mathbf{h}(\mathrm{T}_i^{(n)}, S_\ell),\, \Sigma_{\mathbf{w}}\right)}{\nu^{(\ell)}\left(\mathbf{z}_j^{(\ell)} \mid \mathbf{T}^{(n)}\right)} \tag{81}$$

Recall that

$$\gamma(\mathbf{z} \mid \mathbf{T}) = \sum_{\ell=1}^{s} \nu^{(\ell)}(\mathbf{z} \mid \mathbf{T}) = \sum_{\ell=1}^{s} \left(\sum_{i=1}^{N} p^D(\mathrm{T}_i)\, \mathcal{N}\left(\mathbf{z} | \mathbf{h}\left(\mathrm{T}_i, S_\ell\right), \Sigma_{\mathbf{w}}\right) + \nu_{cl}^{(\ell)}(\mathbf{z}) \right)$$

Thus, $Q\left(\mathbf{T} \mid \mathbf{T}^{(n)}\right)$ can be written as

$$Q\left(\mathbf{T} \mid \mathbf{T}^{(n)}\right) = \sum_{\ell=1}^{s} \left[-\int_{\mathcal{T}} \nu_{cl}^{(\ell)}(\mathbf{z})\, d\mathbf{z} + \sum_{j=1}^{m_\ell} \log\, \nu_{cl}^{(\ell)}(\mathbf{z}_j^{(\ell)})\, \frac{\nu_{cl}^{(\ell)}(\mathbf{z}_j^{(\ell)})}{\nu^{(\ell)}\left(\mathbf{z}_j^{(\ell)} \mid \mathbf{T}^{(n)}\right)} \right] + \sum_{i=1}^{N} \sum_{\ell=1}^{s} \left[\sum_{j=1}^{m_\ell} \log\, p^D(\mathrm{T}_i)\, \mathcal{N}\left(\mathbf{z}_j^{(\ell)} \mid \mathbf{h}(\mathrm{T}_i, S_\ell),\, \Sigma_{\mathbf{w}}\right) \frac{p^D(\mathrm{T}_i^{(n)})\, \mathcal{N}\left(\mathbf{z}_j^{(\ell)} \mid \mathbf{h}(\mathrm{T}_i^{(n)}, S_\ell),\, \Sigma_{\mathbf{w}}\right)}{\nu^{(\ell)}\left(\mathbf{z}_j^{(\ell)} \mid \mathbf{T}^{(n)}\right)} - \int_{\mathcal{T}} p^D(\mathrm{T}_i)\, \mathcal{N}\left(\mathbf{z} | \mathbf{h}\left(\mathrm{T}_i, S_\ell\right), \Sigma_{\mathbf{w}}\right)\, d\mathbf{z} \right] \tag{82}$$

Thus

$$Q\left(\mathbf{T} \mid \mathbf{T}^{(n)}\right) = \sum_{i=1}^{N} Q_i\left(\mathbf{T}_i \mid \mathbf{T}^{(n)}\right) + Q_{cl}\left(\mathbf{T}^{(n)}\right) \tag{83}$$

where

$$Q_i\left(\mathbf{T}_i \mid \mathbf{T}^{(n)}\right) = \sum_{\ell=1}^{s} \left[\sum_{j=1}^{m_\ell} \log\, p^D(\mathrm{T}_i)\, \mathcal{N}\left(\mathbf{z}_j^{(\ell)} \mid \mathbf{h}(\mathrm{T}_i, S_\ell),\, \Sigma_{\mathbf{w}}\right) \times \frac{p^D(\mathrm{T}_i^{(n)})\, \mathcal{N}\left(\mathbf{z}_j^{(\ell)} \mid \mathbf{h}(\mathrm{T}_i^{(n)}, S_\ell),\, \Sigma_{\mathbf{w}}\right)}{\nu^{(\ell)}\left(\mathbf{z}_j^{(\ell)} \mid \mathbf{T}^{(n)}\right)} - \int_{\mathcal{T}} p^D(\mathrm{T}_i)\, \mathcal{N}\left(\mathbf{z} | \mathbf{h}\left(\mathrm{T}_i, S_\ell\right), \Sigma_{\mathbf{w}}\right)\, d\mathbf{z} \right] \tag{84}$$

and

$$Q_{cl}\left(\mathbf{T}^{(n)}\right) = \sum_{\ell=1}^{s} \left[-\int_{\mathcal{T}} \nu_{cl}^{(\ell)}(\mathbf{z})\, d\mathbf{z} + \sum_{j=1}^{m_\ell} \log\, \nu_{cl}^{(\ell)}(\mathbf{z}_j^{(\ell)})\, \frac{\nu_{cl}^{(\ell)}(\mathbf{z}_j^{(\ell)})}{\nu^{(\ell)}\left(\mathbf{z}_j^{(\ell)} \mid \mathbf{T}^{(n)}\right)} \right] \tag{85}$$

This completes the E-step.

6.1.2 M - Step

The M-step maximizes $Q\left(\mathbf{T} \mid \mathbf{T}^{(n)}\right)$ over all feasible $\mathbf{T}$, i.e.,

$$\mathbf{T}^{(n+1)} = \arg\max_{\mathbf{T}} \quad Q\left(\mathbf{T} \mid \mathbf{T}^{(n)}\right). \tag{86}$$

Assuming there is no functional relation between T_i and T_j for $i \neq j$, the required M-step maximum is found by maximizing the expressions $Q_i\left(\mathrm{T}_i \,|\, \mathbf{T}^{(n)}\right)$ separately. Let

$$\mathrm{T}_i^{(n+1)} = \arg\max_{\mathrm{T}_i} \quad Q_i\left(\mathrm{T}_i \,|\, \mathbf{T}^{(n)}\right), \qquad 1 \leq i \leq N. \tag{87}$$

Before we further proceed, note that $\mathcal{N}\left(\mathbf{z}_j^{(\ell)} \,|\, \mathbf{h}\left(\mathrm{T}_i, S_\ell\right), \Sigma_{\mathbf{w}}\right)$ can be written as

$$\mathcal{N}\left(\mathbf{z}_j^{(\ell)} \,|\, \mathbf{h}\left(\mathrm{T}_i, S_\ell\right), \Sigma_{\mathbf{w}}\right) = \frac{1}{\sqrt{\det(2\pi\Sigma_{\mathbf{w}})}} \exp\left[-\frac{1}{2}\left(\mathbf{z}_j^{(\ell)} - \mathbf{h}\left(\mathrm{T}_i, S_\ell\right)\right)^T \times \Sigma_{\mathbf{w}}^{-1}\left(\mathbf{z}_j^{(\ell)} - \mathbf{h}\left(\mathrm{T}_i, S_\ell\right)\right)\right].$$

Thus

$$\log\mathcal{N}\left(\mathbf{z}_j^{(\ell)} \,|\, \mathbf{h}\left(\mathrm{T}_i, S_\ell\right), \Sigma_{\mathbf{w}}\right) = -\log\sqrt{\det(2\pi\Sigma_{\mathbf{w}})} - \frac{1}{2}\left(\mathbf{z}_j^{(\ell)} - \mathbf{h}\left(\mathrm{T}_i, S_\ell\right)\right)^T \Sigma_{\mathbf{w}}^{-1}\left(\mathbf{z}_j^{(\ell)} - \mathbf{h}\left(\mathrm{T}_i, S_\ell\right)\right).$$

Define the weight $\omega_i^{(\ell)}\left(\mathbf{z}_j^{(\ell)} \,|\, \mathrm{T}^{(n)}, \Sigma_{\mathbf{w}}\right)$ as

$$\omega_i^{(\ell)}\left(\mathbf{z}_j^{(\ell)} \,|\, \mathrm{T}^{(n)}, \Sigma_{\mathbf{w}}\right) = \frac{p^D(\mathrm{T}_i^{(n)})\,\mathcal{N}\left(\mathbf{z}_j^{(\ell)} \,|\, \mathbf{h}(\mathrm{T}_i^{(n)}, S_\ell), \Sigma_{\mathbf{w}}\right)}{\nu^{(\ell)}\left(\mathbf{z}_j^{(\ell)} \,|\, \mathbf{T}^{(n)}\right)}. \tag{88}$$

The weight $\omega_i^{(\ell)}\left(\mathbf{z}_j^{(\ell)} \,|\, \mathrm{T}^{(n)}, \Sigma_{\mathbf{w}}\right)$ is the probability that the point $\mathbf{z}_j^{(\ell)}$ is generated by the i-th target given the current estimates $\mathrm{T}^{(n)}$. Now equation 87 can be rewritten as

$$\mathrm{T}_i^{(n+1)} = \arg\max_{\mathrm{T}_i} \quad \sum_{\ell=1}^{s}\left[\sum_{j=1}^{m_\ell} \log\,\mathcal{N}\left(\mathbf{z}_j^{(\ell)} \,|\, \mathbf{h}(\mathrm{T}_i, S_\ell), \Sigma_{\mathbf{w}}\right)\omega_i^{(\ell)}\left(\mathbf{z}_j^{(\ell)} \,|\, \mathrm{T}^{(n)}, \Sigma_{\mathbf{w}}\right) + \sum_{j=1}^{m_\ell} \log\, p^D(\mathrm{T}_i)\,\omega_i^{(\ell)}\left(\mathbf{z}_j^{(\ell)} \,|\, \mathrm{T}^{(n)}, \Sigma_{\mathbf{w}}\right) - \int_{\mathcal{T}} p^D(\mathrm{T}_i)\,\mathcal{N}\left(\mathbf{z}|\mathbf{h}\left(\mathrm{T}_i, S_\ell\right), \Sigma_{\mathbf{w}}\right) d\mathbf{z}\right] \tag{89}$$

Unlike the single-sensor case, here we do not consider two different scenarios based on $p^D(\mathrm{T}_i)$. Here $p^D(\mathrm{T}_i) = I_i$ are assumed to be scalar quantities that need to be estimated along with $\mathbf{T}$.

Here we assume that $p^D(\mathrm{T}_i)$ are scalar quantities, indicated as I_i, that need to be estimated along

with T_i. Thus the optimization problem in equation 89 can be rewritten as

$$\begin{aligned}\mathrm{T}_i^{(n+1)} = \arg\max_{\mathrm{T}_i} \quad & \sum_{\ell=1}^{s}\left[\sum_{j=1}^{m_\ell}\log\mathcal{N}\left(\mathbf{z}_j^{(\ell)} \mid \mathbf{h}(\mathrm{T}_i, S_\ell),\ \Sigma_{\mathbf{w}}\right)\omega_i^{(\ell)}\left(\mathbf{z}_j^{(\ell)} \mid \mathrm{T}^{(n)}, \Sigma_{\mathbf{w}}\right) + \right. \\ & \left. \sum_{j=1}^{m_\ell}\log\ I_i\,\omega_i^{(\ell)}\left(\mathbf{z}_j^{(\ell)} \mid \mathrm{T}^{(n)}, \Sigma_{\mathbf{w}}\right) - \int_{\mathcal{T}} I_i\,\mathcal{N}\left(\mathbf{z}|\mathbf{h}\left(\mathrm{T}_i, S_\ell\right), \Sigma_{\mathbf{w}}\right)\,d\mathbf{z}\right]\end{aligned} \tag{90}$$

$$\begin{aligned}I_i^{(n+1)} = \arg\max_{I_i} \quad & \sum_{\ell=1}^{s}\left[\sum_{j=1}^{m_\ell}\log\mathcal{N}\left(\mathbf{z}_j^{(\ell)} \mid \mathbf{h}(\mathrm{T}_i, S_\ell),\ \Sigma_{\mathbf{w}}\right)\omega_i^{(\ell)}\left(\mathbf{z}_j^{(\ell)} \mid \mathrm{T}^{(n)}, \Sigma_{\mathbf{w}}\right) + \right. \\ & \left. \sum_{j=1}^{m_\ell}\log\ I_i\,\omega_i^{(\ell)}\left(\mathbf{z}_j^{(\ell)} \mid \mathrm{T}^{(n)}, \Sigma_{\mathbf{w}}\right) - \int_{\mathcal{T}} I_i\,\mathcal{N}\left(\mathbf{z}|\mathbf{h}\left(\mathrm{T}_i, S_\ell\right), \Sigma_{\mathbf{w}}\right)\,d\mathbf{z}\right]\end{aligned} \tag{91}$$

From equation 90, $\mathrm{T}_i^{(n+1)}$ satisfies the necessary condition:

$$\begin{aligned}\sum_{\ell=1}^{s}\left[\sum_{j=1}^{m_\ell}\omega_i^{(\ell)}\left(\mathbf{z}_j^{(\ell)} \mid \mathrm{T}^{(n)}, \Sigma_{\mathbf{w}}\right)\Sigma_{\mathbf{w}}^{-1}\left[\mathbf{z}_j^{(\ell)} - \mathbf{h}\left(\mathrm{T}_i, S_\ell\right)\right]\nabla_{\mathrm{T}_i}\mathbf{h}\left(\mathrm{T}_i, S_\ell\right) - \right. \\ \left. \int_{\mathcal{T}} I_i\,\mathcal{N}\left(\mathbf{z}|\mathbf{h}\left(\mathrm{T}_i, S_\ell\right), \Sigma_{\mathbf{w}}\right)\Sigma_{\mathbf{w}}^{-1}\left[\mathbf{z} - \mathbf{h}\left(\mathrm{T}_i, S_\ell\right)\right]\nabla_{\mathrm{T}_i}\mathbf{h}\left(\mathrm{T}_i, S_\ell\right)\,d\mathbf{z}\right] = 0\end{aligned} \tag{92}$$

The above condition can be rewritten as

$$\begin{aligned}\sum_{\ell=1}^{s}\left\{\Sigma_{\mathbf{w}}^{-1}\left[\sum_{j=1}^{m_\ell}\omega_i^{(\ell)}\left(\mathbf{z}_j^{(\ell)} \mid \mathrm{T}^{(n)}, \Sigma_{\mathbf{w}}\right)\left[\mathbf{z}_j^{(\ell)} - \mathbf{h}\left(\mathrm{T}_i, S_\ell\right)\right] - \right.\right. \\ \left.\left. \int_{\mathcal{T}} I_i\,\mathcal{N}\left(\mathbf{z}|\mathbf{h}\left(\mathrm{T}_i, S_\ell\right), \Sigma_{\mathbf{w}}\right)\left[\mathbf{z} - \mathbf{h}\left(\mathrm{T}_i, S_\ell\right)\right]\,d\mathbf{z}\right]\nabla_{\mathrm{T}_i}\mathbf{h}\left(\mathrm{T}_i, S_\ell\right)\right\} = 0\end{aligned} \tag{93}$$

Based on the assumption $\int_{\mathcal{T}}\mathcal{N}\left(\mathbf{z}|\mathbf{h}\left(\mathrm{T}_i, S_\ell\right), \Sigma_{\mathbf{w}}\right)\mathbf{z}\,d\mathbf{z} \approx \mathbf{h}\left(\mathrm{T}_i, S_\ell\right)$ and $\int_{\mathcal{T}}\mathcal{N}\left(\mathbf{z} \mid \mathbf{h}(\mathrm{T}_i),\ \Sigma_{\mathbf{w}}\right)\,d\mathbf{z} \approx 1$, the EM updates $\mathrm{T}_i^{(n+1)}$ is calculated as the solution to the equation

$$\sum_{\ell=1}^{s}\sum_{j=1}^{m_\ell}\omega_i^{(\ell)}\left(\mathbf{z}_j^{(\ell)} \mid \mathrm{T}^{(n)}, \Sigma_{\mathbf{w}}\right)\mathbf{z}_j^{(\ell)} = \sum_{\ell=1}^{s}\sum_{j=1}^{m_\ell}\omega_i^{(\ell)}\left(\mathbf{z}_j^{(\ell)} \mid \mathrm{T}^{(n)}, \Sigma_{\mathbf{w}}\right)\mathbf{h}\left(\mathrm{T}_i^{(n+1)}, S_\ell\right) \tag{94}$$

Due to the nonlinear nature of the above equation, there exist no closed form solution to above equation. There exist several ways to solve the above equations such as Newton's root finding algorithm. On the other hand, one can also solve equation 94 directly using a search method or a gradient descent method.

On the other hand, $I_i^{(n+1)}$ satisfies the necessary condition:

$$\sum_{\ell=1}^{s}\left(\sum_{j=1}^{m_\ell}\omega_i^{(\ell)}\left(\mathbf{z}_j^{(\ell)}\mid \mathrm{T}^{(n)},\Sigma_{\mathbf{w}}\right)\frac{1}{I_i}-\int_{\mathcal{T}}\mathcal{N}\left(\mathbf{z}|\mathbf{h}\left(\mathrm{T}_i,S_\ell\right),\Sigma_{\mathbf{w}}\right)\,d\mathbf{z}\right)=0 \tag{95}$$

Thus

$$I_i^{(n+1)}=\frac{\displaystyle\sum_{\ell=1}^{s}\sum_{j=1}^{m_\ell}\omega_i^{(\ell)}\left(\mathbf{z}_j^{(\ell)}\mid \mathrm{T}^{(n)},\Sigma_{\mathbf{w}}\right)}{\displaystyle\sum_{\ell=1}^{s}\int_{\mathcal{T}}\mathcal{N}\left(\mathbf{z}|\mathbf{h}\left(\mathrm{T}_i,S_\ell\right),\Sigma_{\mathbf{w}}\right)\,d\mathbf{z}} \tag{96}$$

6.2 AIC-Based Model Selection

The previous subsection provides an EM approach to estimate the target locations given the number of targets. Presented in this approach is an information theoretic approach to select the appropriate model, i.e., the number of targets. Similar to the single-sensor scenario, here we use the AIC to select the appropriate number of targets.

As seen in the E-step, the probability $p\left(\boldsymbol{\psi}^{(1)},\ldots,\boldsymbol{\psi}^{(s)}\mid\mathbf{T}\right)$ can be written as

$$p\left(\boldsymbol{\psi}^{(1)},\ldots,\boldsymbol{\psi}^{(s)}\mid\mathbf{T}\right)=\prod_{\ell=1}^{s}\left[\exp\left(-\int_{\mathcal{T}}\nu^{(\ell)}(\mathbf{z}\mid\mathbf{T})\,d\mathbf{z}\right)\prod_{j=1}^{m_\ell}\nu^{(\ell)}\left(\mathbf{z}_j^{(\ell)}\mid\mathbf{T}\right)\right] \tag{97}$$

Since $\int_{\mathcal{T}}\nu^{(\ell)}(\mathbf{z}\mid\mathbf{T})\,d\mathbf{z}=\widehat{N}$, where $\widehat{N}$ is a candidate for the number of targets, the likelihood $\mathfrak{L}\left(\widehat{\mathbf{T}},\widehat{N}\mid\boldsymbol{\psi}^{(1)},\ldots,\boldsymbol{\psi}^{(s)}\right)$ can be written as

$$\mathfrak{L}\left(\widehat{\mathbf{T}},\widehat{N}\mid\boldsymbol{\psi}^{(1)},\ldots,\boldsymbol{\psi}^{(s)}\right)=\prod_{\ell=1}^{s}\left[\exp\left(-\widehat{N}\right)\prod_{j=1}^{m_\ell}\nu^{(\ell)}\left(\mathbf{z}_j^{(\ell)}\mid\widehat{\mathbf{T}}\right)\right] \tag{98}$$

Now following the information given in subsection 3.2.1, the AIC can be calculated as

$$\mathrm{AIC}=-2\log\mathfrak{L}\left(\widehat{\mathbf{T}},\widehat{N}\mid\boldsymbol{\psi}^{(1)},\ldots,\boldsymbol{\psi}^{(s)}\right)+6\widehat{N}. \tag{99}$$

Therefore, the proposed approach would select several different candidates for $\widehat{N}$ and solve the corresponding localization problem using the EM algorithm. Afterwards, the AIC associated with each model is calculated and the model corresponding to the lowest AIC is selected as the estimated model.

7. Multi-Sensor Example

Consider a scenario, where there are four targets ($N = 4$) located at

$$\mathrm{T} = \left(\begin{bmatrix} 298 \\ -5 \end{bmatrix}, \begin{bmatrix} 250 \\ 7 \end{bmatrix}, \begin{bmatrix} 267 \\ -17 \end{bmatrix}, \begin{bmatrix} 310 \\ 18 \end{bmatrix} \right),$$

and three sensors located at

$$\begin{bmatrix} S_{x_1} \\ S_{y_1} \end{bmatrix} = \begin{bmatrix} 10 \\ -0.5 \end{bmatrix}, \begin{bmatrix} S_{x_2} \\ S_{y_2} \end{bmatrix} = \begin{bmatrix} -15 \\ -2.5 \end{bmatrix} \ \& \ \begin{bmatrix} S_{x_3} \\ S_{y_3} \end{bmatrix} = \begin{bmatrix} -15 \\ 2 \end{bmatrix}.$$

Following the setup presented in section 5., the measurement intensity corresponding to the $\ell-$th sensor is given as

$$\nu^{(\ell)}\left(\mathbf{z} \,|\, \mathbf{T}\right) = \sum_{i=1}^{N} p^{D}(\mathrm{T}_i)\, \mathcal{N}\left(\mathbf{z} | \mathbf{h}\left(\,\mathrm{T}_i, S_\ell\,\right), \Sigma_{\mathbf{w}}\right) + \nu_{cl}^{(\ell)}(\mathbf{z}).$$

For simplifying the problem here we assume, $\nu_{cl}^{(\ell)}(\mathbf{z})$ is the same for all $\ell \in \{1, 2, 3\}$ and $p^{D}(\mathrm{T}_i) = I_i$. The known measurement covariance matrix is $\Sigma_{\mathbf{w}} = \begin{bmatrix} 9 & 0 \\ 0 & 5 \times 10^{-3} \end{bmatrix}$, i.e., the range standard deviation amounts to 3 m and the bearing standard deviation amounts to 4^{o}. The I_i's are given as

$$I_{1:4} = \{0.5525, 1.8399, 1.2119, 0.3957\}$$

and the clutter intensity is given as

$$\nu_{cl}(\mathbf{z}) = 0.0122\mathcal{N}\left(\mathbf{z} \,|\, \mathbf{h}\left(\begin{bmatrix} 281.25 \\ 0.75 \end{bmatrix}\right), \begin{bmatrix} 900 & 0 \\ 0 & 0.4874 \end{bmatrix}\right).$$

Thus the intensity corresponding to the PPP consists of all measurements among the three sensors is given as

$$\gamma(\mathbf{z}) = \sum_{\ell=1}^{3} \left(\sum_{i=1}^{4} I_i\, \mathcal{N}\left(\mathbf{z} | \mathbf{h}\left(\,\mathrm{T}_i, S_\ell\,\right), \Sigma_{\mathbf{w}}\right) + \nu_{cl}^{(\ell)}(\mathbf{z}) \right).$$

In order to evaluate the performance of the algorithm, 200 MC runs were conducted. For each run, the number of measurements for each sensor is determined by sampling from the Poisson

distribution

$$p_M(m) \approx \frac{(4)^m}{m!} \exp\{-4\}.$$

For the ℓ-th sensor, the m_ℓ measurements are obtained from the mixture pdf

$$\frac{1}{4.0122}\left[\sum_{i=1}^{4} I_i \mathcal{N}\left(\mathbf{z}|\mathbf{h}\left(\mathrm{T}_i, S_\ell\right), \Sigma_{\mathbf{w}}\right) + 0.0122\mathcal{N}\left(\mathbf{z} \,|\, \mathbf{h}\left(\begin{bmatrix}281.25\\0.75\end{bmatrix}\right), \begin{bmatrix}900 & 0\\0 & 0.4874\end{bmatrix}\right)\right]$$

with mixing probabilities $\{0.1377, 0.4586, 0.3021, 0.0986, 0.0030\}$. After obtaining the measurements for all three sensors, the proposed EM algorithm is executed for each model using the appropriate initial condition selected from the following set:

$$\left\{\begin{bmatrix}320\\20\end{bmatrix}, \begin{bmatrix}250\\0\end{bmatrix}, \begin{bmatrix}295\\0\end{bmatrix}, \begin{bmatrix}265\\-10\end{bmatrix}, \begin{bmatrix}275\\5\end{bmatrix}, \begin{bmatrix}300\\15\end{bmatrix}\right\}.$$

Here we consider the following five models:

$$N_1 = 2, N_2 = 3, N_3 = 4, N_4 = 5, \text{ and } N_5 = 6.$$

For each model the AIC is then calculated according to the information given in subsection 6.2 and the model corresponding to the minimum AIC is selected as the correct model.

Here we use the OSPA metric to assess the performance and accuracy of the proposed localization algorithm (*30*). To be specific, we use the OSPA metric of order 1 with cut-off value 100.

Given in figure 4 is the histogram obtained from the MC runs for the number of measurements for all three sensors. Note that the histogram for the number of measurements resembles that of a Poisson pdf with a rate of four.

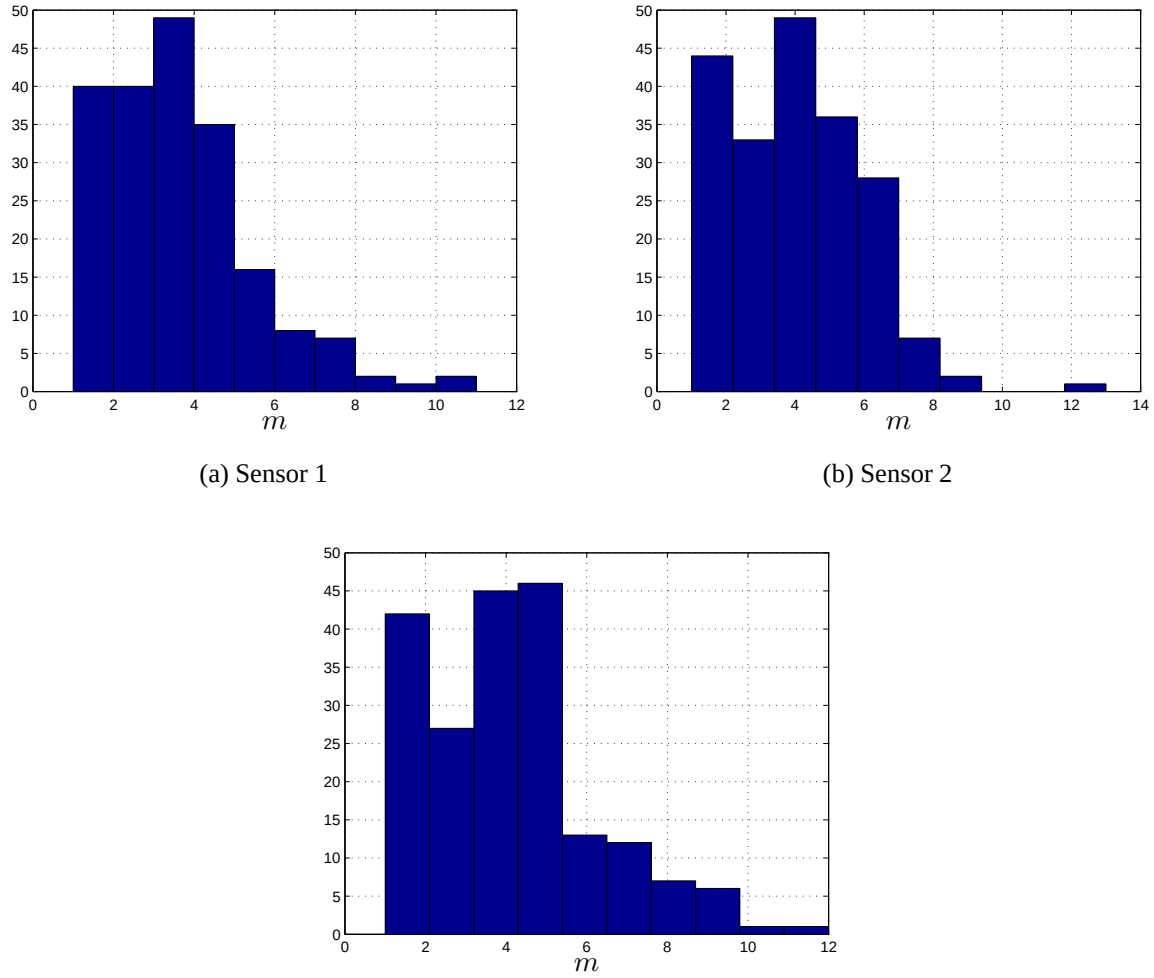

(a) Sensor 1

(b) Sensor 2

(c) Sensor 3

Figure 4. Histogram for number of measurements.

Figure 5a contains the histogram obtained from the MC runs for the number of estimated targets. The histogram for the estimated number of targets clearly indicates that there are four targets. Figure 5b contains the OSPA metric obtained for each MC runs. Note that the OSPA metric around the 100 mark indicates the MC runs with a cardinality error of one while the OSPA metric around the 200 mark indicates the MC runs with a cardinality error of two. Note that most of the metrics are well below 50 indicating no cardinality error and accurate localization.

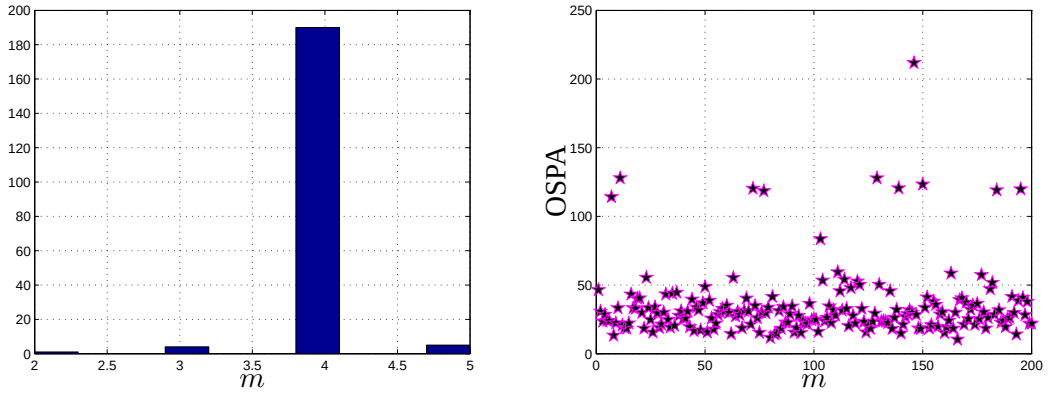

(a) Estimated number of targets

(b) OSPA metric for each MC runs

Figure 5. Estimated number of targets and OSPA metric for each MC runs.

Given in figure 6 is the localization results obtained for one of the MC trials. For the numerical results presented in figure 6, $m_1 = 6$, $m_2 = 2$, $m_3 = 5$ and the measurement are

$$\begin{bmatrix} 286.5969 & 6.2309 \\ 240.8335 & 0.0081 \\ 259.9712 & 6.2273 \\ 302.0675 & 0.0577 \\ 256.8199 & 6.2335 \\ 288.3582 & 6.2747 \end{bmatrix}, \begin{bmatrix} 331.4559 & 0.0351 \\ 310.6632 & 6.2480 \end{bmatrix}, \begin{bmatrix} 313.1043 & 0.0071 \\ 267.7569 & 6.2744 \\ 283.0506 & 6.1852 \\ 321.8741 & 0.0963 \\ 262.4796 & 0.0491 \end{bmatrix}.$$

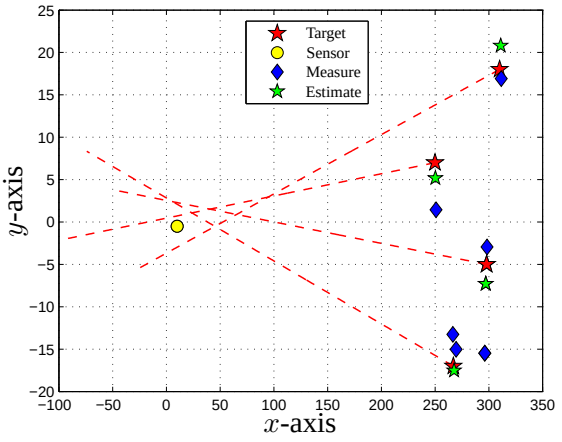

(a) Sensor 1

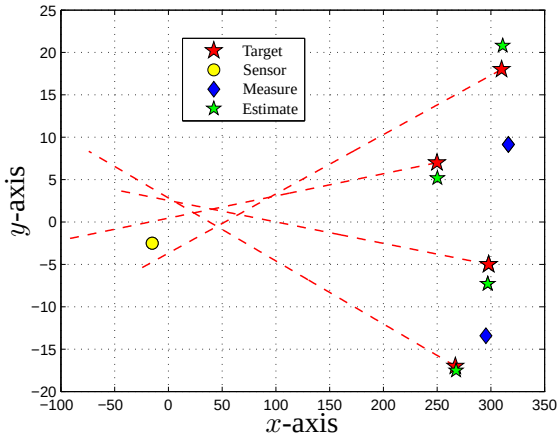

(b) Sensor 2

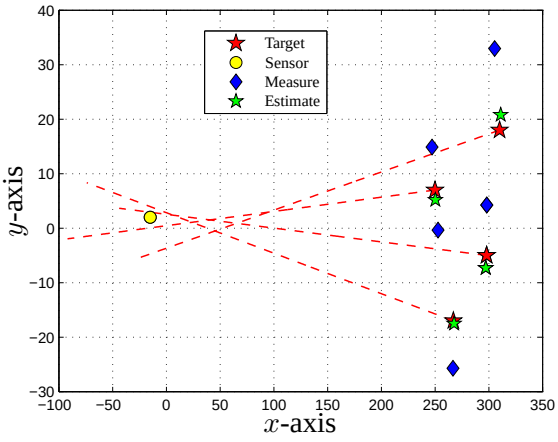

(c) Sensor 3

Figure 6. Individual sensor measurements and EM solutions.

For all MC runs, five different models are selected and the correct model is selected as the one with lowest AIC score. Thus the parameter estimates are $\widehat{N} = 4$ and

$$\widehat{\mathrm{T}} = \left(\begin{bmatrix} 297.1037 \\ -7.3038 \end{bmatrix}, \begin{bmatrix} 311.0966 \\ 20.7981 \end{bmatrix}, \begin{bmatrix} 267.6813 \\ -17.5251 \end{bmatrix}, \begin{bmatrix} 250.3221 \\ 5.1730 \end{bmatrix} \right).$$

The fused solution along with the individual measurements are given in figure 7, where the fused solutions are displayed as green stars. As shown in figure 6, sensor one yields six measurements (indicated as blue diamonds), sensor two yields two measurements (indicated as cyan squares),

and sensor three yields four measurements (indicated as magenta triangles).

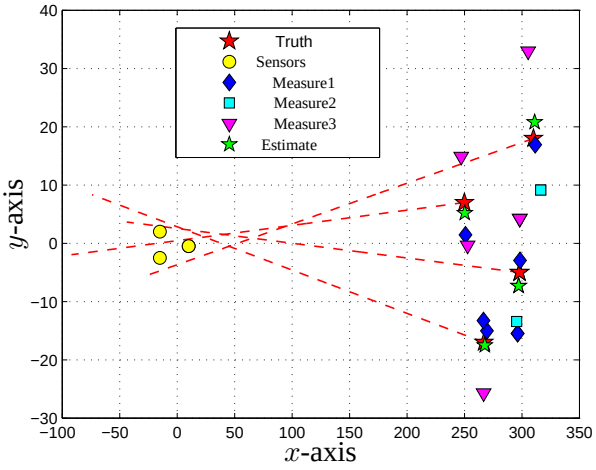

Figure 7. Multi-sensor fused solution.

8. Experimental Results

This section presents the implementation of the proposed algorithm for multi-shooter localization using a network of acoustic GDSs. The individual GDSs are composed of a passive array of microphones that is able to localize a gunfire event by measuring the direction of arrival for both the acoustic wave generated by the muzzle blast and the shockwave generated by the supersonic bullet (*2–5*). After detecting a gunfire, the individual sensors report their solution, usually in the form of range and bearing to the shooter locations relative to the sensor, along with their orientation and GPS positions to a central node over a communication network. At the central node, the individual sensor solutions are fused along with the GPS positions to yield a highly accurate, geo-rectified solution. More details on shooter localization using a network of acoustic GDSs can be found in references (*31–37*).

Experiments were conducted for the quad symmetric sensor formation given in figure 8 using a sensor network composed of nine sensors. The sensor pattern spreads over 25 m front to back. In figure 8, the shooter position is marked by a red human figure, and the shot line is marked by a translucent red line. The GPS locations of the three shooter positions are given in table 3.

Figure 8. Quad symmetric sensor formation.

Table 3. Shooter Locations.

Shooter Position	GPS - East (m)	GPS - North (m)
Shooter Position 1	283309	4709539
Shooter Position 2	283270	4709567
Shooter Position 3	283337	4709632

The sensor locations and headings correspond to the quad symmetric formation are given in table 4.

Table 4. Sensor locations and heading for quad symmetric formation.

Sensor	GPS - East (m)	GPS - North (m)	Heading (deg)
SW1	283130	4709427	40
SW2	283129	4709434	39
SW3	283165	4709401	31
UGS1	283133	4709431	39
UGS2	283169	4709398	30
UGS3	283168	4709405	31
VM1	283127	4709431	40
VM2	283172	4709402	30
VM3	283177	4709395	29

Here, 30 shots were fired for each shooter position. For each run, the number of measurements

reported by each sensor is modeled as the Poisson distribution

$$p_M(m) \approx \frac{(3)^m}{m!} \exp\{-3\}.$$

Following the formulation presented in section 5., the m_ℓ measurements obtained for the ℓ-th sensor are modeled as i.i.d. samples from the mixture pdf

$$\frac{1}{3.0122}\left[\sum_{i=1}^{3} I_i \mathcal{N}\left(\mathbf{z}|\mathbf{h}\left(\mathrm{T}_i, S_\ell\right), \Sigma_{\mathbf{w}}\right) + 0.0122\mathcal{N}\left(\mathbf{z}\,|\,\mathbf{h}\left(\begin{bmatrix}4709579.33\\ 283305.33\end{bmatrix}\right), \begin{bmatrix}1000 & 0\\ 0 & 1.0\end{bmatrix}\right)\right]$$

with mixing probabilities $\{0.4378, 0.4853, 0.0728, 0.0041\}$. The covariance associated with individual measurements are obtained from the confidence weights provided by the sensors (*32*). After obtaining the measurements for all nine sensors, the proposed EM algorithm is executed for each model using the appropriate initial condition selected. Here we consider the following four models:

$$N_1 = 2, N_2 = 3, N_3 = 4, \text{ and } N_4 = 5.$$

For each model the AIC is then calculated according to the information given in subsection 6.2 and the model corresponding to the minimum AIC is selected as the correct model.

Similar to the previous results, here also we used the OSPA metric of order 1 with cut-off value 100 to assess the performance and accuracy of the proposed localization algorithm (*30*).

Given in figure 9 is the histogram obtained from the MC runs for the number of measurements for all nine sensors. Note that the histogram for the number of measurements resembles that of a Poisson pdf with a rate of three.

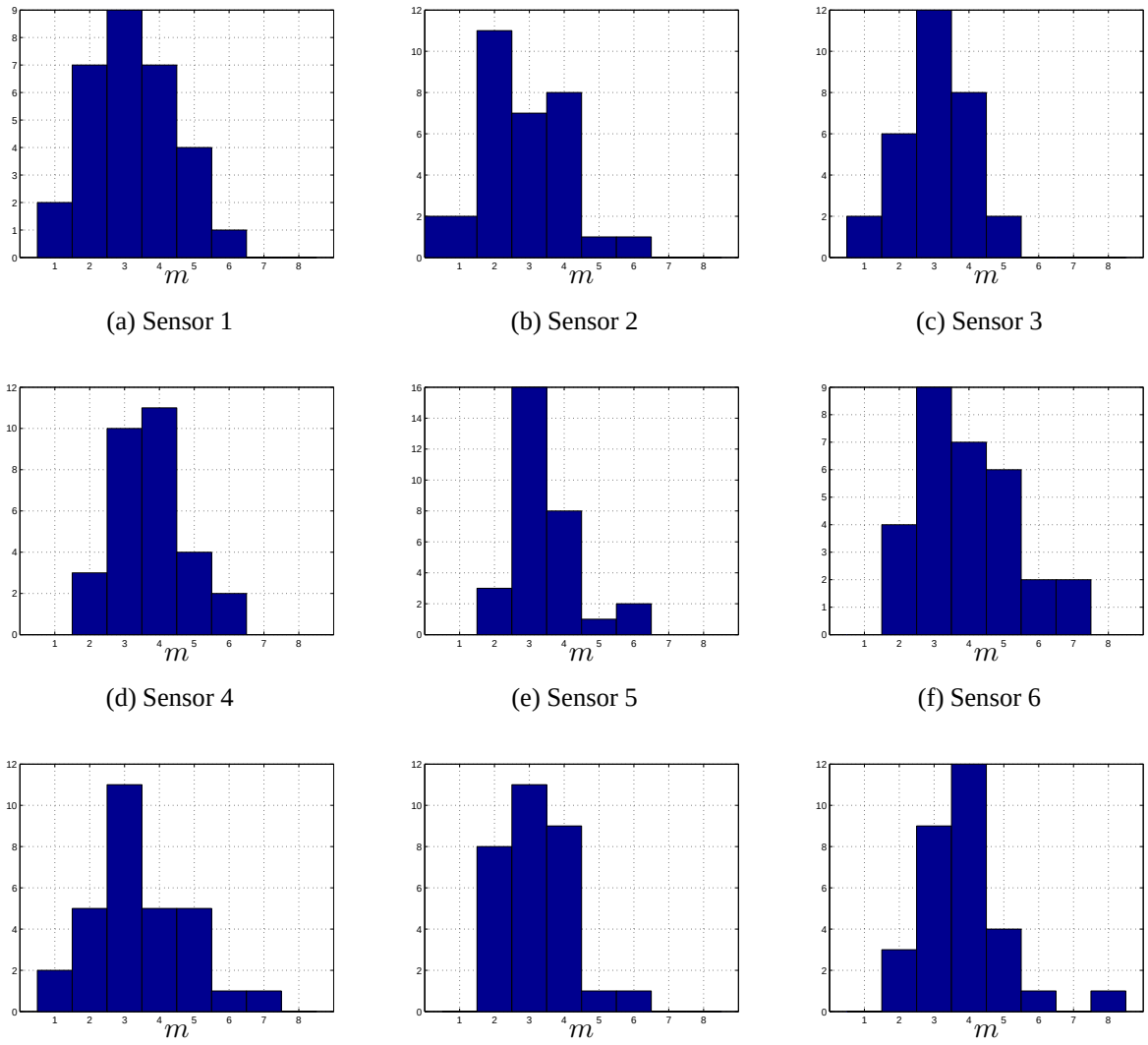

(a) Sensor 1 (b) Sensor 2 (c) Sensor 3

(d) Sensor 4 (e) Sensor 5 (f) Sensor 6

(g) Sensor 7 (h) Sensor 8 (i) Sensor 9

Figure 9. Histogram for number of measurements for each experimental runs.

Figure 10 contains the histogram obtained from the 30 experimental runs for the number of estimated targets. The histogram for the estimated number of targets clearly indicates that there are three targets.

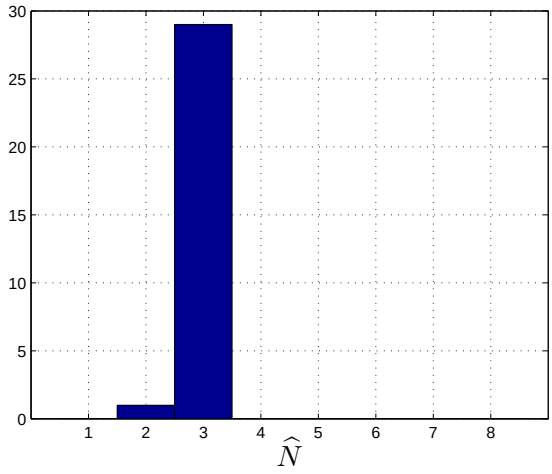

Figure 10. Estimated number of targets.

Figure 11 contains the OSPA metric obtained for each experimental runs. Note that most of the metrics are well below 20 indicating no cardinality error and very accurate localization.

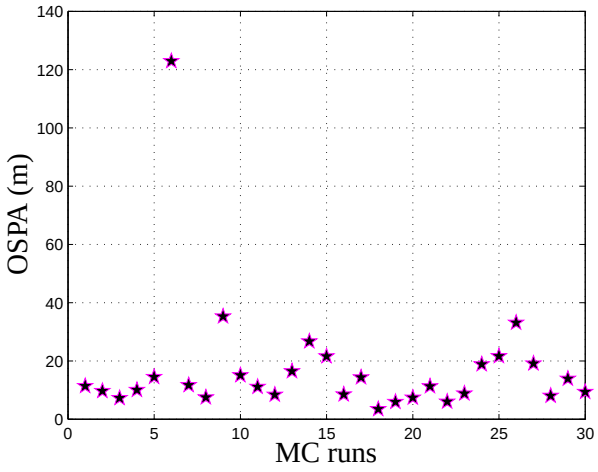

Figure 11. OSPA metric for experimental runs.

Given in figure 12 is the localization results obtained for one of the experimental trials. For the numerical results presented in figure 6, $m_1 = 2$, $m_2 = 6$, $m_3 = 1$, $m_4 = 4$, $m_5 = 4$, $m_6 = 2$, $m_7 = 4$, $m_8 = 3$, and $m_9 = 3$. In figure 12, the measurements obtained for each sensors are

denoted as blue diamonds, the true shooter locations are denoted as red stars, the sensor location is denoted as yellow circles, and the estimated shooter locations are represented as green stars.

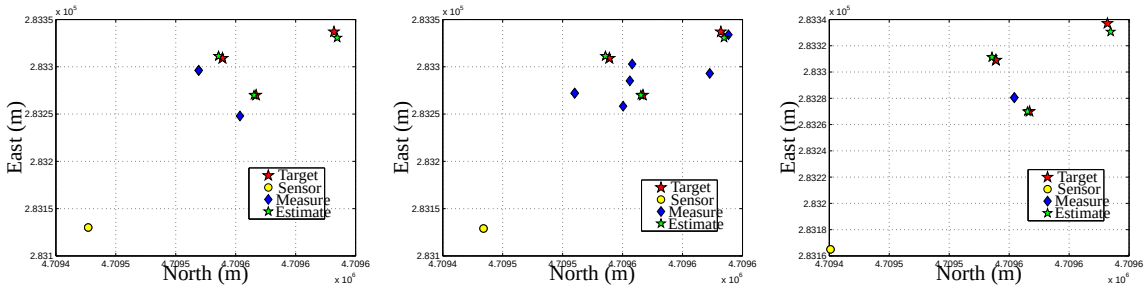

(a) Sensor 1 (b) Sensor 2 (c) Sensor 3

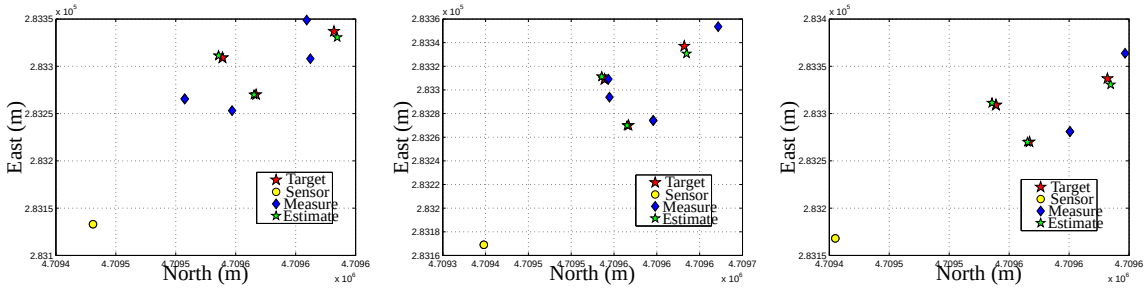

(d) Sensor 4 (e) Sensor 5 (f) Sensor 6

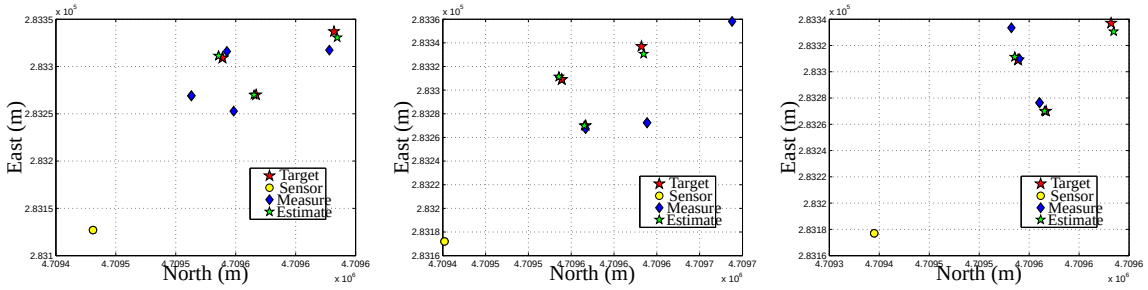

(g) Sensor 7 (h) Sensor 8 (i) Sensor 9

Figure 12. Experimental results for individual sensor measurements and EM solutions.

The fused solution along with the individual measurements are given in figure 13, where the fused solutions are displayed as green stars. As shown in figure 13, the fused solution is more accurate compared to the individual measurements.

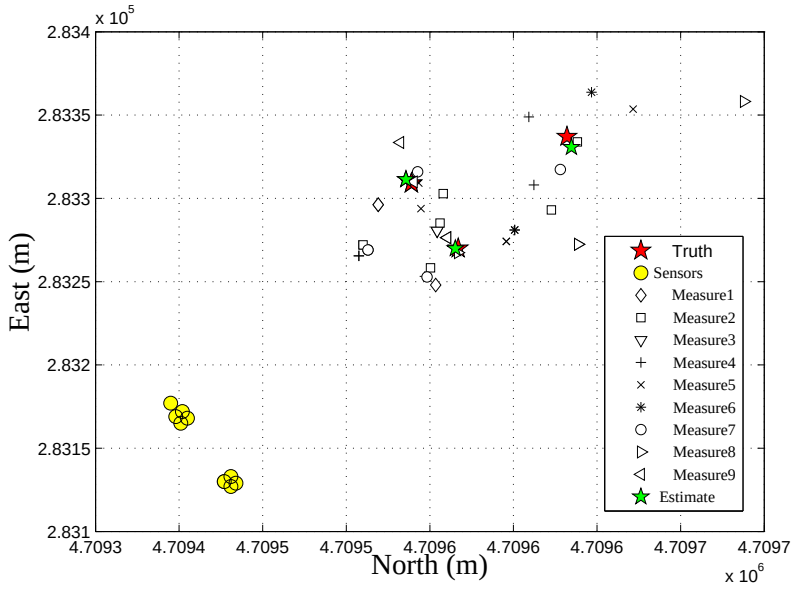

Figure 13. Experimental result for multi-sensor fusion.

9. Conclusion

This report presents the finite point process approach to the multi-target localization problem for the single-sensor as well as multi-sensor scenario. Here it is assumed that target identification is not possible, and therefore, no association between the measurements and targets are available. Furthermore, the number of targets in the surveillance region is unknown, and due to the limited range of the sensors, missed detections can occur and the presence of clutter can induce false alarms. Here we propose an EM algorithm to estimate the target locations while the information criterion, AIC, is used to estimate the number of targets. The preliminary implementation of the proposed algorithm on synthetic data produced accurate results. Implementation of the proposed algorithm on experimental data obtained for the multi-shooter localization problem further confirms the numerical results. Here we use the optimal subpattern assignment metric of order 1 with a cut-off value of 100 to assess the performance of the localization algorithm. As the results given in sections 7. and 8. indicate, the finite point process approach is able to accurately estimate the number of targets and their locations in the presence of clutter and missed detection. Future work will include decreasing the sensitivity of the proposed algorithm to the initial guess with the use of multiple-thread search and deterministic annealing EM algorithm (*38*). The current scheme can also benefit from a systematic approach for selecting potential target models.

10. References

1. George, J.; Kaplan, L. Shooter Localization using a Wireless Sensor Network of Soldier-Worn Gunfire Detection Systems. *Journal of Advances in Information Fusion* **2013**, *8* (1), 15-32.

2. Makinen, T.; Pertila, P. Shooter localization and bullet trajectory, caliber, and speed estimation based on detected firing sounds. *Applied Acoustics* **2010**, *71* (10), 902-913.

3. Kaplan, L.; Damarla, T.; Pham, T. QoI for passive acoustic gunfire localization. In *5th IEEE International Conference on Mobile Ad Hoc and Sensor Systems, MASS,* Atlanta GA, Sep.-Oct. 2008.

4. Duckworth, G. L.; Gilbert, D. C.; Barger, J. E. Acoustic counter-sniper system. In *Proceedings of Society of Photo-Optical Instrumentation Engineers (SPIE) Conference*; Vol. 2938, Boston, MA, Nov. 1997.

5. Bédard, J.; Paré, S. Ferret: A small arms' fire detection system: Localization concepts. In *Proceedings of Society of Photo-Optical Instrumentation Engineers (SPIE) Conference*; Vol. 5071, Orlando, FL, Apr. 2003.

6. Blackman, S. Multiple hypothesis tracking for multiple target tracking. *Aerospace and Electronic Systems Magazine, IEEE* **2004**, *19* (1), 5-18.

7. Vermaak, J.; Godsill, S.; Perez, P. Monte Carlo filtering for multi target tracking and data association. *Aerospace and Electronic Systems, IEEE Transactions on* **2005**, *41* (1), 309-332.

8. Bar-Shalom, Y.; Tse, E. Tracking in a cluttered environment with probabilistic data association. *Automatica* **1975**, *11* (5), 451-460.

9. T. Fortmann, Y. B.-S.; Scheffe, M. Sonar tracking of multiple targets using joint probabilistic data association. *IEEE J. Ocean. Eng.* **1983**, *8* (3), 173-183.

10. Reid, D. An algorithm for tracking multiple targets. *Automatic Control, IEEE Transactions on* **1979**, *24* (6), 843 - 854.

11. Bar-Shalom, Y.; Fortmann, T. *Tracking and Data Association*; Academic Press: New York, 1988.

12. Perlovsky, L. I. Cramer-Rao bound for tracking in clutter and tracking multiple objects. *Pattern Recognition Letters* **1997**, *18* (3), 283 - 288.

13. Garcia-Fernandez, A.; Morelande, M.; Grajal, J. Multitarget Simultaneous Localization and Mapping of a Sensor Network. *Signal Processing, IEEE Transactions on* **2011**, *59* (10), 4544 - 4558.

14. Montemerlo, M.; Thrun, S.; Koller, D.; Wegbreit, B. FastSLAM: a factored solution to the simultaneous localization and mapping problem. In *Eighteenth national conference on Artificial intelligence*, American Association for Artificial Intelligence: Menlo Park, CA, USA, 2002.

15. Jensfelt, P.; Kristensen, S. Active global localization for a mobile robot using multiple hypothesis tracking. *Robotics and Automation, IEEE Transactions on* **2001**, *17* (5), 748 - 760.

16. Mahler, R. Multitarget Bayes filtering via first-order multitarget moments. *Aerospace and Electronic Systems, IEEE Transactions on* **2003**, *39* (4), 1152-1178.

17. Lin, L.; Bar-Shalom, Y.; Kirubarajan, T. Track labeling and PHD filter for multitarget tracking. *Aerospace and Electronic Systems, IEEE Transactions on* **2006**, *42* (3), 778-795.

18. Vo, B.-N.; Singh, S.; Doucet, A. Sequential Monte Carlo methods for multitarget filtering with random finite sets. *Aerospace and Electronic Systems, IEEE Transactions on* **2005**, *41* (4), 1224-1245.

19. Vo, B.-N.; Ma, W.-K. The Gaussian Mixture Probability Hypothesis Density Filter. *Signal Processing, IEEE Transactions on* **2006**, *54* (11), 4091-4104.

20. Clark, D.; Bell, J. Convergence results for the particle PHD filter. *Signal Processing, IEEE Transactions on* **2006**, *54* (7), 2652-2661.

21. Clark, D.; Vo, B.-N. Convergence Analysis of the Gaussian Mixture PHD Filter. *Signal Processing, IEEE Transactions on* **2007**, *55* (4), 1204-1212.

22. Vo, B.-N.; Singh, S.; Ma, W.-K. Tracking multiple speakers using random sets. In *Acoustics, Speech, and Signal Processing, 2004. Proceedings. (ICASSP '04). IEEE International Conference on*; Vol. 2, 2004.

23. Ma, W.-K.; Vo, B.-N.; Singh, S.; Baddeley, A. Tracking an unknown time-varying number of speakers using TDOA measurements: a random finite set approach. *Signal Processing, IEEE Transactions on* **2006**, *54* (9), 3291-3304.

24. Xiaodong, L.; Linhu, Z.; Zhengxin, L. Probability hypothesis densities for multi-sensor, multi-target tracking with application to acoustic sensors array. In *Advanced Computer Control (ICACC), 2010 2nd International Conference on*; Vol. 5, 2010.

25. Deming, R. W.; Perlovsky, L. I. Concurrent multi-target localization, data association, and navigation for a swarm of flying sensors. *Information Fusion* **2007**, *8* (3), 316 - 330.

26. Carevic, D. Automatic Estimation of Multiple Target Positions and Velocities Using Passive TDOA Measurements of Transients. *Signal Processing, IEEE Transactions on* **2007**, *55* (2), 424-436.

27. Carevic, D. Multitarget Detection and Estimation Based on Passive Multilateral TDOAs of Transient Signals. *Signal Processing, IEEE Transactions on* **2008**, *56* (1), 418-424.

28. Streit, R. Poisson Point Processes: Imaging, Tracking, and Sensing. In , Springer: New York, NY, 2010; Chapter 2-3, pp 11–80.

29. Akaike, H. A new look at the statistical model identification. *Automatic Control, IEEE Transactions on* **1974**, *19* (6), 716 - 723.

30. Schuhmacher, D.; Vo, B.-T.; Vo, B.-N. A Consistent Metric for Performance Evaluation of Multi-Object Filters. *Signal Processing, IEEE Transactions on* **2008**, *56* (8), 3447 - 3457.

31. George, J.; Kaplan, L. Shooter localization using soldier-worn gunfire detection systems. In *Proceedings of the 12th International Conference on Information Fusion (FUSION)*, Chicago, IL, July 2011.

32. George, J.; Kaplan, L. M.; Kozick, R.; Deligeorges, S. Multi-Sensor Data Fusion using Soldier-Worn Gunfire Detection Systems. In *Proc. MSS Battlespace Acoustic and Magnetic Sensors (BAMS)*, Washington, DC, Oct. 2011.

33. Damarla, T.; Kaplan, L.; Whipps, G. Sniper Localization Using Acoustic Asynchronous Sensors. *Sensors Journal, IEEE* **2010**, *10* (9), 1469-1478.

34. Lindgren, D.; Wilsson, O.; Gustafsson, F.; Habberstad, H. Shooter Localization in Wireless Microphone Networks. *EURASIP Journal on Advances in Signal Processing* **2010**, *2010* (6), 1-25.

35. Lindgren, D.; Wilsson, O.; Gustafsson, F.; Habberstad, H. Shooter localization in wireless sensor networks. In *Proceedings of the 12th International Conference on Information Fusion (FUSION)*, Seattle, WA, July 2009.

36. Volgyesi, P.; Balogh, G.; Nadas, A.; Nash, C. B.; Ledeczi, A. Shooter localization and weapon classification with soldier-wearable networked sensors. In *Proceedings of the 5th international conference on Mobile systems, applications and services*, New York, NY, June 2007.

37. Ledeczi, A.; Volgyesi, P.; Maroti, M.; Simon, G.; Balogh, G.; Nadas, A.; Kusy, B.; Dora, S.; Pap, G. Multiple simultaneous acoustic source localization in urban terrain. In *Fourth International Symposium on Information Processing in Sensor Networks, IPSN*, Los Angeles, CA, Apr. 2005.

38. Takada, M.; Nakano, R. Multi-thread search with deterministic annealing EM algorithm. In *Neural Networks, 2002. IJCNN '02. Proceedings of the 2002 International Joint Conference on*; Vol. 1, 2002.

INTENTIONALLY LEFT BLANK.

NO. OF COPIES	ORGANIZATION
1 (PDF)	DEFENSE TECHNICAL INFORMATION CTR DTIC OCA
2 (PDF)	DIRECTOR US ARMY RESEARCH LAB RDRL CIO LL IMAL HRA MAIL & RECORDS MGMT
1 (PDF)	GOVT PRINTG OFC A MALHOTRA
5 (PDF)	DIRECTOR US ARMY RESEARCH LAB RDRL SES A JEMIN GEORGE LANCE M. KAPLAN TIEN PHAM NASSY SROUR GENE T. WHIPPS